Clim Dyn (2015) 44:585–607
DOI 10.1007/s00382-015-2468-6

The double ITCZ bias in CMIP5 models: interaction between SST, large-scale circulation and precipitation

Boutheina Oueslati · Gilles Bellon

Received: 6 May 2013 / Accepted: 2 January 2015 / Published online: 18 January 2015
© Springer-Verlag Berlin Heidelberg 2015

Abstract The double intertropical convergence zone (ITCZ) bias still affects all the models that participate to CMIP5 (Coupled Model Intercomparison Project, phase 5). As an ensemble, general circulation models have improved little between CMIP3 and CMIP5 as far as the double ITCZ is concerned. The present study proposes a new process-oriented metrics that provides a robust statistical relationship between atmospheric processes and the double ITCZ bias, additionally to the existing relationship between the sea surface temperature (SST) and the double ITCZ bias. The SST contribution is examined using the THR-MLT index (Bellucci et al. in J Clim 5:1127–1145, 2010), which combines biases on the representation of local SSTs and the SST threshold leading to the onset of ascent in the double ITCZ region. As a metrics of a model's bias in simulating the interaction between circulation and precipitation, we propose to use the Combined Precipitation Circulation Error (CPCE). It is computed as the quadratic error on the contribution of each vertical regime to the total precipitation over the tropical oceans. CPCE is a global measure of the circulation-precipitation coupling that characterizes the model physical parameterizations rather than the regional characteristics of the eastern Pacific. A linear regression analysis shows that most of the double ITCZ spread among CMIP5 coupled ocean–atmosphere models is attributed to SST biases, and that the precipitation large-scale dynamics relationship explains a significant fraction of the bias in these models, as well as in the atmosphere-only models.

B. Oueslati (✉) · G. Bellon
Centre National de Recherches Météorologiques (CNRS)/Météo-France, 42, Avenue Gaspard Coriolis, 31057 Toulouse, France
e-mail: boutheina.oueslati@u-bourgogne.fr

B. Oueslati
Centre de Recherches de Climatologie, Biogéosciences, CNRS/Université de Bourgogne, 6, Bd Gabriel, 21000 Dijon, France

Keywords Double ITCZ · Atmospheric dynamics · Coupled ocean–atmosphere feedbacks

1 Introduction

Most current general circulation models (GCMs) still suffer from the double intertropical convergence zone (ITCZ) problem (Mechoso et al. 1995; Dai 2006). They fail to simulate a single ITCZ north of the equator year-round. Instead, they produce a second maximum of precipitation south of the equator in the Pacific and Atlantic oceans during at least half of the year, whereas it is only observed in the eastern Pacific during boreal spring (Hubert et al. 1969; Zhang 2001). The double ITCZ bias affecting the central Pacific can be connected to the simulation of a too-zonally elongated South Pacific convergence zone (SPCZ).

Both atmospheric and coupled ocean–atmosphere processes play an important role in controlling the ITCZ location. The sea surface temperature (SST) affects convection by supplying heat and moisture to the atmospheric column through the turbulent surface fluxes, and by creating low-level convergence through its gradients (Lindzen and Nigam 1987; Back and Bretherthon 2008; Oueslati and Bellon 2013a). The spatial distribution of SST is however poorly simulated in coupled ocean–atmosphere GCMs (OAGCMs), with a positive SST bias over the southeastern Pacific and an excessive equatorial cold tongue extending too far west in the Pacific. These biases are attributed to coupled ocean–atmosphere feedbacks such as the SST-wind-induced surface fluxes feedback, the SST-stratus feedback and the SST gradient-trade wind feedback associated with vertical upwelling (Lin 2007).

Together with the SST's control, atmospheric mechanisms are crucial in determining the ITCZ location. Deep

convection can force a large-scale circulation by modifying the pressure gradients through moist diabatic processes (Gill 1980; Oueslati and Bellon 2013a). Vice-versa, large-scale circulation can promote or suppress convection through ascending and subsiding motions, modifying the vertical heating profile and the moisture-convection feedbacks (e.g. Lau et al. 1997; Hirota et al. 2011; Oueslati and Bellon 2013b), so that the feedbacks between dynamics and moist thermodynamics are instrumental in controlling the precipitation pattern. Based on the conditional instability of the second kind (CISK) theory (Charney 1971) and the associated wave-CISK mechanisms (Holton et al. 1971; Lindzen 1974; Hess et al. 1993), early studies emphasized the role of the positive feedback between convection and large-scale convergence to explain the ITCZ location. Atmospheric dynamics promote convection through large-scale upward motions favouring atmospheric instability and moisture convergence, but it can also suppress convection through large-scale subsidence (Lau et al. 1997; Xie et al. 2010). Subsequent studies highlighted the importance of the interaction between convection and its large-scale environment on the basis of the quasi-equilibrium theory (Arakawa and Schubert 1974; Emanuel 1994). According to this theory, both dynamical and thermodynamical processes control the convective activity and, thus, the ITCZ location. In particular, Numaguti (1993) showed that the ITCZ structure is sensitive to the surface-flux parametrization and Liu et al. (2010) associated the double ITCZ obtained in aquaplanet settings with the wind-evaporation feedback. The quasi-equilibrium theory *per se* does not provide a systematic mechanism of interaction between precipitation and dynamics.

The ITCZ pattern is very sensitive to the deep-convection scheme and the associated parameters because they determine the response of the convection to given large-scale environment, and also because they control the dynamic response to convection through the vertical profile of convective heating. Rain re-evaporation (Bacmeister et al. 2006), cold top and downdrafts (Oueslati and Bellon 2013a) and lateral entrainment (Chikira 2010; Hirota et al. 2011; Oueslati and Bellon 2013b) can all have an impact on the precipitation pattern. In particular, sensitivity studies to convective entrainment using the CNRM-CM5 hierarchy of models show that, in that model, the double ITCZ bias is associated with biases in the probability density function (PDF) of mid-tropospheric vertical wind resulting from feedbacks between dynamics and convection (Oueslati and Bellon 2013b).

The purpose of this study is to quantify the respective roles of SST and large-scale dynamics in the Pacific double ITCZ problem in OAGCMs and, when available, corresponding atmosphere-only GCMs (AGCMs) participating in CMIP5 (Coupled Model Intercomparison Project, phase 5). We attempt to propose process-oriented metrics to evaluate the contribution of the atmospheric processes to the double ITCZ bias and to the intermodel spread of this bias, compared to the contribution of the coupled ocean–atmosphere processes. Proposing such diagnostics help find linkage between model biases and physical processes. This approach is particularly useful for model developers because it facilitates model evaluation and improvement. The SST contribution is quantified using the metrics developed by Bellucci et al. (2010). The large-scale atmospheric contribution is examined using the regime sorting methodology developed by Bony et al. (2004). These two contributions are quantified based on a linear regression analysis. Using this statistical method, we attempt to show that the double ITCZ bias is associated not only with biases of the local SST (Bellucci et al. 2010) but also with the systematic errors on the representation of the coupling between precipitation and large-scale atmospheric circulation.

The paper is structured as follows. In Sect. 2, we introduce the models used for this study. In Sect. 3, we document the CMIP5 OAGCMs systematic errors in tropical precipitation. Section 4 quantifies the role of SST and associated coupled ocean–atmosphere feedbacks in the double ITCZ bias. Section 5 investigates the contribution of precipitation/dynamics interaction to this systematic bias. The respective roles of the coupled ocean–atmosphere processes and atmospheric precipitation/dynamics processes are quantified in Sect. 6. Summary and conclusions are given in Sect. 7.

2 Data

This study uses monthly mean data for both observations and model simulations. The observations (referred to as OBS in figure legends) include the Global Precipitation Climatology Project (GPCP) version 2 precipitation dataset (Adler et al. 2003), the global Hadley Centre Global Sea Ice and Sea Surface Temperature (HadISST) analyses (Rayner et al. 2003) and the 40-year ECMWF Re-analysis (ERA40) for the mid-tropospheric vertical pressure velocity ω_{500} fields. Observations and reanalyses are provided for the 1979–2001 period. The use of monthly data is suitable in this study to avoid the synoptic variability of daily data and the unreliable vertical velocity in reanalyses at this time scale.

Model simulations are used over the 1979–1999 period. We use the reference historical simulations performed for CMIP5 (referred to as CMIP). They are currently available for 17 OAGCMs at the time of this study. In addition, we use the corresponding atmosphere-only simulations (commonly referred to as Atmospheric Model Intercomparison Project (AMIP) simulations), with prescribed SST

and interactive continental surfaces. These AMIP simulations are available for 13 AGCMs out of the 17 OAGCMs. Table 1 summarizes the characteristics of the models used in this study with their names and acronyms, their horizontal and vertical resolutions and a brief description of their deep convection schemes. For simplicity, we refer to each model by the name of its institution in figure legends.

3 Precipitation patterns in CMIP5 OAGCMs

3.1 Annual mean precipitation

Figure 1 shows the annual mean precipitation over the period 1979–1999 from GPCP v2 precipitation dataset Adler et al. (2003) and 17 CMIP5 OAGCMs. All the models still produce the double ITCZ bias to some extent, with excessive precipitation south of the equator in the Pacific Ocean: the SPCZ is too-zonally elongated and a spurious ITCZ is simulated in the Eastern Pacific. In some models (e.g., GISS-E2-R and MRI-CGCM3), a double ITCZ pattern is also evident over the tropical Atlantic Ocean. Other model deficiencies still persist, including the excessive precipitation over the Maritime Continent, Indian Ocean, and within the Pacific ITCZ, and the insufficient precipitation over the equator in the Pacific.

To quantify the double ITCZ bias over the tropical Pacific in GCMs, Bellucci et al. (2010) proposed a Southern ITCZ (SI) index, computed as the annual mean precipitation over the Double ITCZ region (20 S-0 , 100 -150 W, referred to as the DI region). The results of this study and the interpretation of the mechanisms controlling the ITCZ location are not sensitive to the latitudinal extent of the DI region. Figure 2 compares the SI index calculated for CMIP3 and CMIP5 models. It appears clearly that the double ITCZ bias is still present in all models. Only four modelling groups out of the 13 common ones between CMIP3 and CMIP5 improved their simulation of the annual mean precipitation in the southeastern Pacific. For the IPSL-CM5A, MPI-ESM-LR and CNRM-CM5, the improvement results partly from an increase in resolution: the vertical resolution has been increased in IPSL-CM5A-LR and MPI-ESM-LR compared to the models in the CMIP3 generation, the horizontal resolution has been increased in CNRM-CM5 and both the horizontal and vertical resolutions have been increased in IPSL-CM5A-MR, but the convection parametrization in these models has not been significantly altered. IPSL-CM5B-LR and NCAR-CCSM4 also show an improvement in the SI index, and it can be explained by improvements in the existing parametrization of deep convection (Grandpeix and Lafore 2010; Grandpeix et al. 2010 for IPSL-CM5B-LR; Neale et al. 2008 for NCAR-CCSM4). In particular, in NCAR-CCSM4, two changes were made within the previous Zhang and McFarlane (1995) convection scheme. One is the inclusion of the effects of deep convection in the momentum equation (Richter and Rasch 2008). The second one is a modification of the calculation of convective available potential energy (CAPE), that has been reformulated to include more realistic dilution effects through an explicit representation of entrainment (Neale et al. 2008). Taking into account entrainment in cumulus parametrization strengthens the sensitivity of convection to the free-tropospheric humidity, resulting in a more constrained but vigorous precipitation (Neale et al. 2008; Oueslati and Bellon 2013b). Compared to its CMIP3 version, MRI-CGCM3 no longer uses monthly climatological flux corrections, and this could explain the increase in SI index shown in Fig. 2.

Figure 3 shows the SI index computed from both CMIP5 OAGCMs and AGCMs. The double ITCZ bias is present in AMIP simulations. However, for the majority of models, its amplitude is smaller than in CMIP simulations. This is particularly the case of BCC-CSM1-1, GFDL-ESM2M and MRI-CGCM3. It appears, therefore, that coupled ocean–atmosphere feedbacks are still responsible for most of the double ITCZ bias in the East Pacific, maybe even more so than in the previous generation of models (Lin 2007). This confirms that alleviating the double ITCZ bias in AGCMs is insufficient to solve the double ITCZ problem in OAGCMs as was suggested by the spread in the sensitivity of AGCMs and OAGCMs to convective entrainment (Oueslati and Bellon 2013b).

3.2 Mean seasonal cycle

Figures 4 and 5 show the seasonal cycle of monthly precipitation averaged over two longitude sectors of the Pacific ocean from GPCP and for CMIP5 models. The seasonal cycle of the precipitation in the Eastern Pacific (80W–120W) has improved in some OAGCMs, as shown in Fig. 4, compared to Dai (2006) and De Szoeke and Xie (2008). De Szoeke and Xie (2008) divided the CMIP3 models into three main categories based on their seasonal cycle of precipitation. The first collects models displaying a persistent double ITCZ error in which rain persists too long in the Southern Hemisphere. The second collects models with an ITCZ and an SST maxima that cross the equator following the seasonal shift of the insolation maximum. The third group collects models that are in qualitative agreement with the observed seasonal cycle, with the dominance of the northern ITCZ from May to December and the double ITCZ structure in March and April (see Fig. 4 GPCP). This classification is still relevant for CMIP5 models, with improvements in some models. In particular, CNRM-CM5 and INMCM4 no longer simulate a double ITCZ year-round (De Szoeke and

Table 1 List of models analyzed in this study

Modeling groups	IPCC ID	Atmospheric resolution	Deep convection scheme	Closure/trigger
National Centre for Atmospheric Research (NCAR)	CCSM4	$\simeq 0.9° \times 1.25°$-L26	Revised Zhang and McFarlane (1995): Neale et al. (2008), Richter and Rasch (2008)	"Dilute" CAPE
Canadian Centre for Climate Modeling and Analysis (CCCMA)	CanESM2 CanAM4 (AGCM)	T63-L35	Zhang and McFarlane (1995)	CAPE
LASG-IAP/LASG, Institute of Atmospheric Physics, Chinese Academy of Sciences (IAP)	FGOALS-g2	$\simeq 2.5° \times 4°$-L26	Zhang and McFarlane (1995)	CAPE
NASA Goddard Institute for Space Studies (GISS)	GISS-E2-R	$\simeq 2° \times 2.5°$-L40	Del Genio and Yao (1993)	A cloud base neutral buoyancy/Parcel buoyancy
Beijing Climate Centre, China Meteorological Administration (BCC)	BCC-CSM1-1	T42-L26	Revised Zhang and McFarlane (1995) Zhang and Mu (2005):	CAPE/relative humidity threshold
Centre National de Recherches Meteorologiques (CNRM)	CNRM-CM5	T127-L31	Bougeault (1985)	Kuo/conditional instability
Atmosphere and Ocean Research Institute (The University of Tokyo), National Institute for Environmental Studies, and Japan Agency for Marine-Earth Science and Technology (MIROC)	MIROC5	T85-L40	Chikira and Sugiyama (2010)	Prognostic convective kinetic energy
Met Office Hadley Centre (MOHC)	HadGEM2-ES HadGEM2-A (AGCM)	$\simeq 1.25° \times 1.875°$-L38	Revised Gregory and Rowntree (1990) + Buoyancy-dependent Detrainment (Derbyshire et al. 2011)	Stability-dependent mass-flux/parcel buoyancy
Commonwealth Scientific and Industrial Research Organisation in collaboration with the Queensland Climate Change Centre of Excellence (CSIRO)	CSIRO-Mk3-6-0	T63-L18	Gregory and Rowntree (1990)	Stability-dependent mass-flux/parcel buoyancy
Meteorological Research Institute (MRI)	MRI-CGCM3	TL159-L48	Pan and Randall (1998)	Prognostic convective kinetic energy
Geophysical Fluid Dynamics Laboratory (GFDL)	GFDL-ESM2M GFDL-HIRAM- C360 (AGCM)	$\simeq 2.5° \times 2°$-L24	Moorthi and Suarez (1992)	CAPE/relative humidity Threshold
Max Planck Institute for Meteorology (MPI)	MPI-ESM-LR	$\simeq 1.9° \times 1.9°$-L47	Nordeng (1994)	CAPE
Institute for Numerical Mathematics (INM)	INMCM4	$\simeq 1.5° \times 2°$-L21	Betts (1986)	CAPE
Institut Pierre-Simon Laplace (IPSL)	IPSL-CM5A-LR	$\simeq 1.9° \times 3.75°$-L39	Emanuel (1991)	CAPE
	IPSL-CM5A-MR	$\simeq 1.25° \times 2.5°$-L39	Emanuel (1991)	CAPE
	IPSL-CM5B-LR	$\simeq 1.9° \times 3.75°$-L39	Grandpeix and Lafore (2010) Grandpeix et al. (2010)	Available lifting power/available lifting energy
Norwegian Climate Centre (NCC)	NorESM1-M	$\simeq 1.8° \times 2.5°$-L26	Zhang and McFarlane (1995)	CAPE

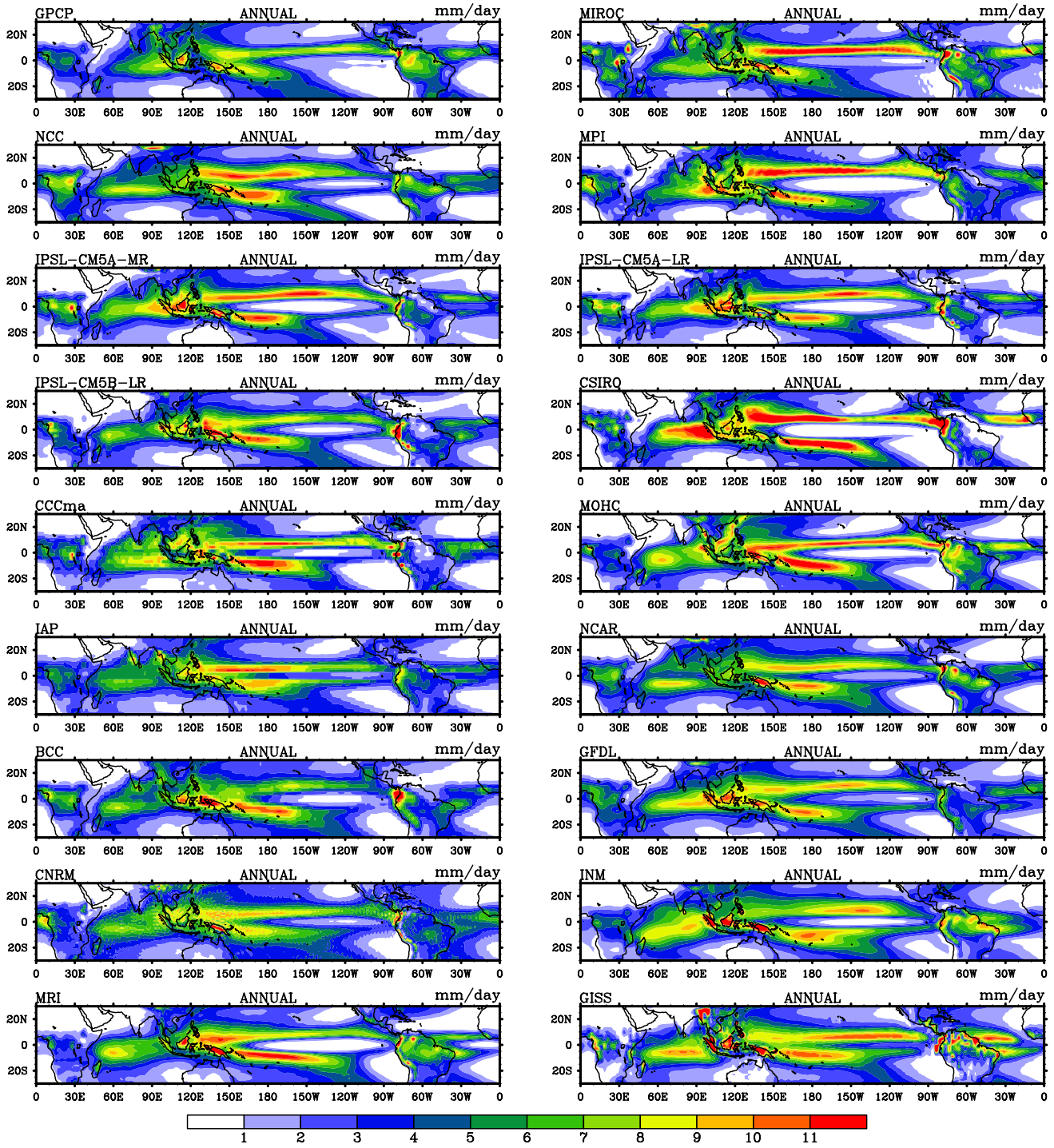

Fig. 1 Annual precipitation (1979–1999) from GPCP data and 17 CMIP5 OAGCMs

Xie 2008), but simulate a single ITCZ that moves across the equator following the solar forcing, similarly to the majority of CMIP5 models (IPSL-CM5, NCC-NorESM1-M, MPI-ESM-LR, CCCma-CanESM2,. . .). Two models (GISS-E2-R and IAP-FGOALS-g2) still exhibit a persistent double ITCZ error, with precipitation persisting year-round in the Southern Hemisphere. Three models (MIROC5, CSIRO-Mk3-6-0 and MOHC-HadGEM2-ES) reproduce qualitatively the observed seasonal cycle of precipitation. In MOHC-HadGEM2-ES, however, the southern ITCZ is much more intense than in the observations ($\simeq$9 mm day^{-1}), explaining the increase of the SI index from CMIP3 to CMIP5 (see Fig. 2).

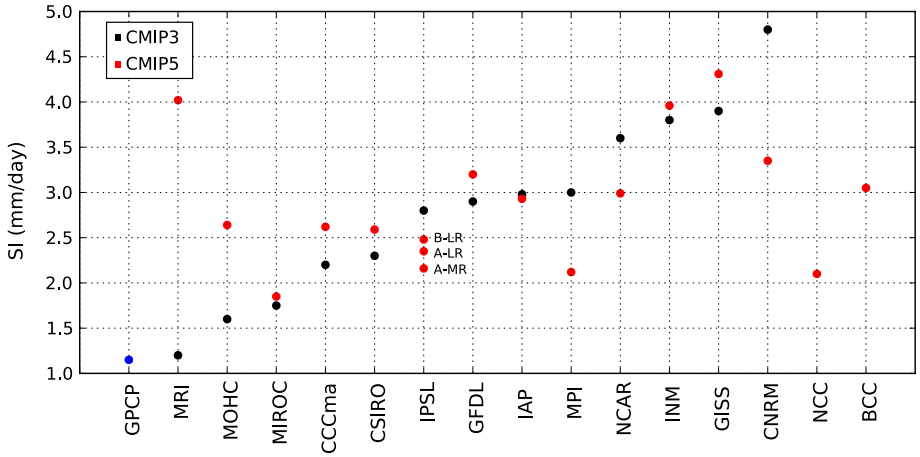

Fig. 2 Southern ITCZ (SI) index for observations, CMIP3 and CMIP5 OAGCMs

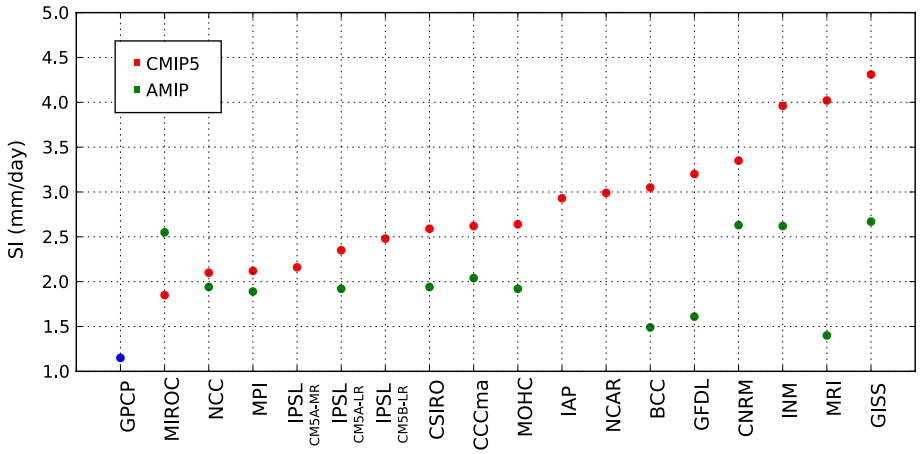

Fig. 3 SI index for CMIP5 AGCMs (AMIP) and OAGCMs (CMIP)

Over the Central Pacific (130W–170W), most of the models produce a persistent double ITCZ error with a southern rainbelt present throughout the year (see Fig. 5). Only few models simulate qualitatively the seasonal cycle of the ITCZ, with no southern rainbelt in boreal summer (MIROC5, IPSL-CM5). However, it still persists too long compared to observations. In this region, the bias of simulated precipitation is in fact connected to the simulation of a too-zonally elongated SPCZ.

4 Coupled ocean–atmosphere contribution to the double ITCZ bias

In the tropics, organized convective activity is often collocated with warm SSTs. Warm SSTs cause large turbulent surface fluxes that increase low-level moist static energy and thus create an environment favorable for convection. The SST also has a non local dynamical effect through its gradient that creates low-level convergence (Lindzen and Nigam 1987; Back and Bretherthon 2008; Oueslati and Bellon 2013a). The modulation of the SST through coupled ocean–atmosphere feedbacks is therefore crucial to the precipitation pattern.

In this section, we focus on the role of the local SST control on precipitation, and particularly on the double ITCZ bias in southeastern Pacific in CMIP5 models, using the metrics proposed by Bellucci et al. (2010). This metrics is defined in the DI region (20°S–0°, 100°–150°W) and identified as a critical parameter controlling the strength of the DI systematic bias in CMIP3 OAGCMs. In this section we attempt to verify its relevance in CMIP5 OAGCMs and try to understand the information provided by THR-MLT, in OAGCMs and AGCMs.

4.1 Description of the Bellucci index THR-MLT

The Bellon et al. (2010) methodology is based on a regime-sorting analysis applied to SST in the DI region. The PDF of SST (bins of 0.5 C) is computed over the DI region (see Fig. 6a). The SST corresponding to the maximum of the PDF is identified as the most likely temperature (MLT) of the ocean surface in the DI region (Bellucci et al. 2010). MLT allows to determine whether a model is warm or

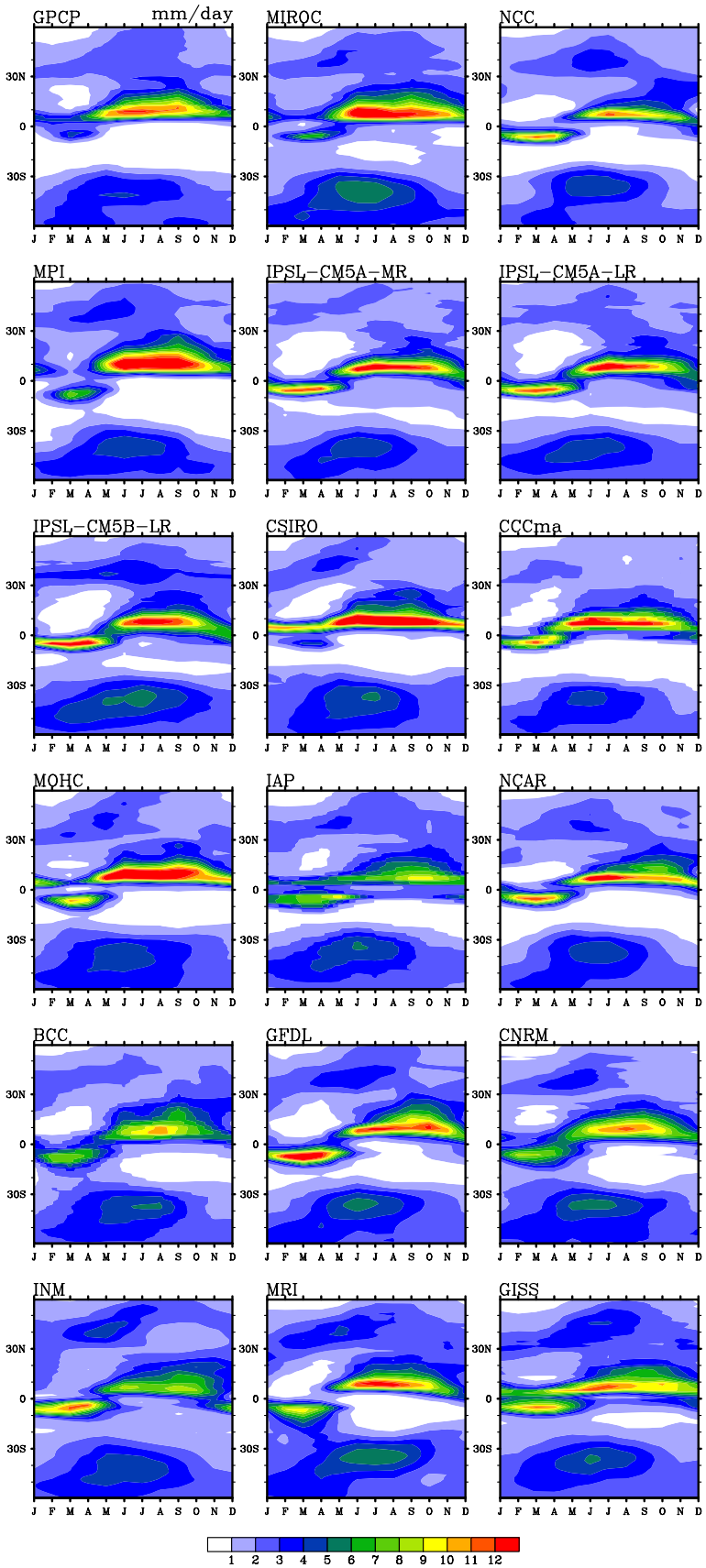

Fig. 4 Seasonal cycle of precipitation in eastern Pacific (80W–120W) for GPCP data and CMIP5 OAGCMs

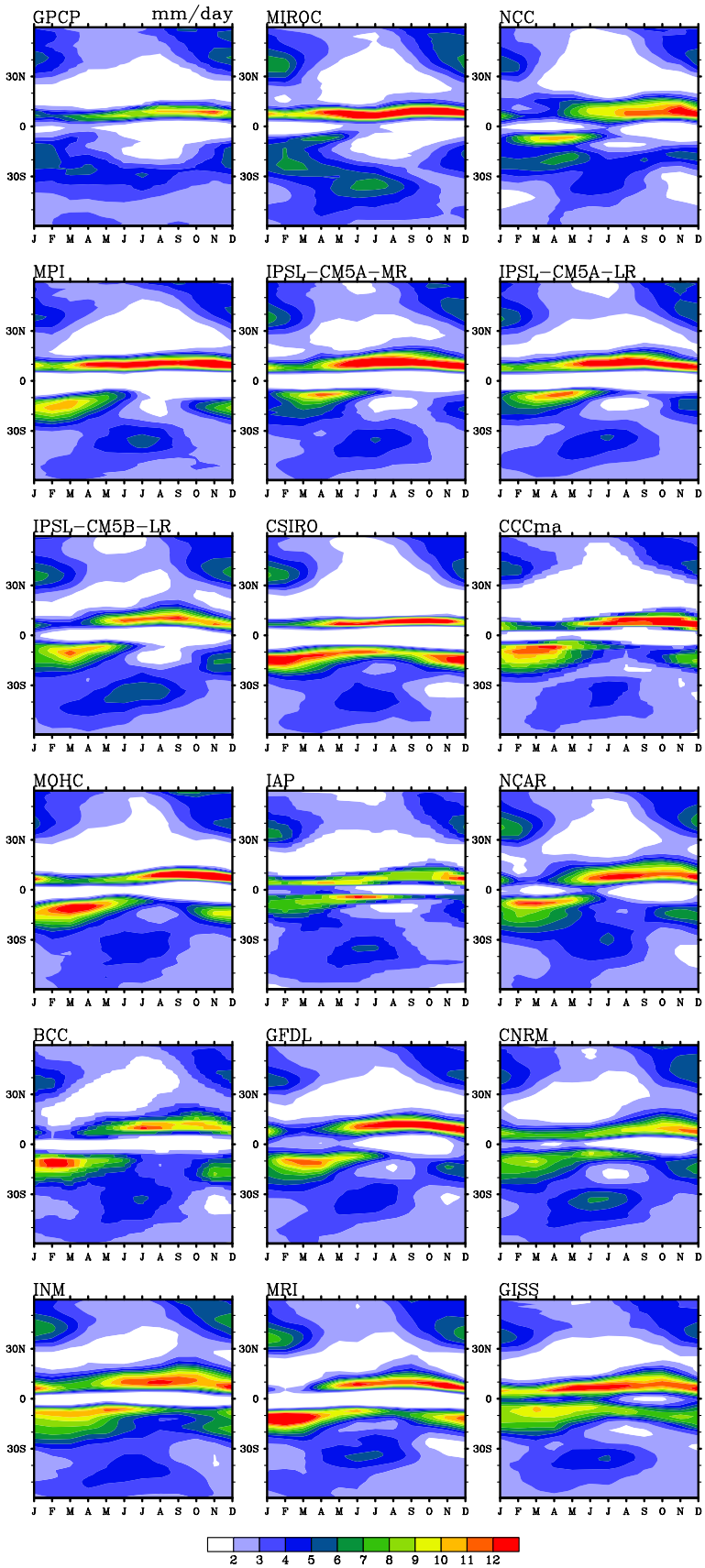

Fig. 5 Seasonal cycle of precipitation in central Pacific (130W–170W) for GPCP data and CMIP5 OAGCMs

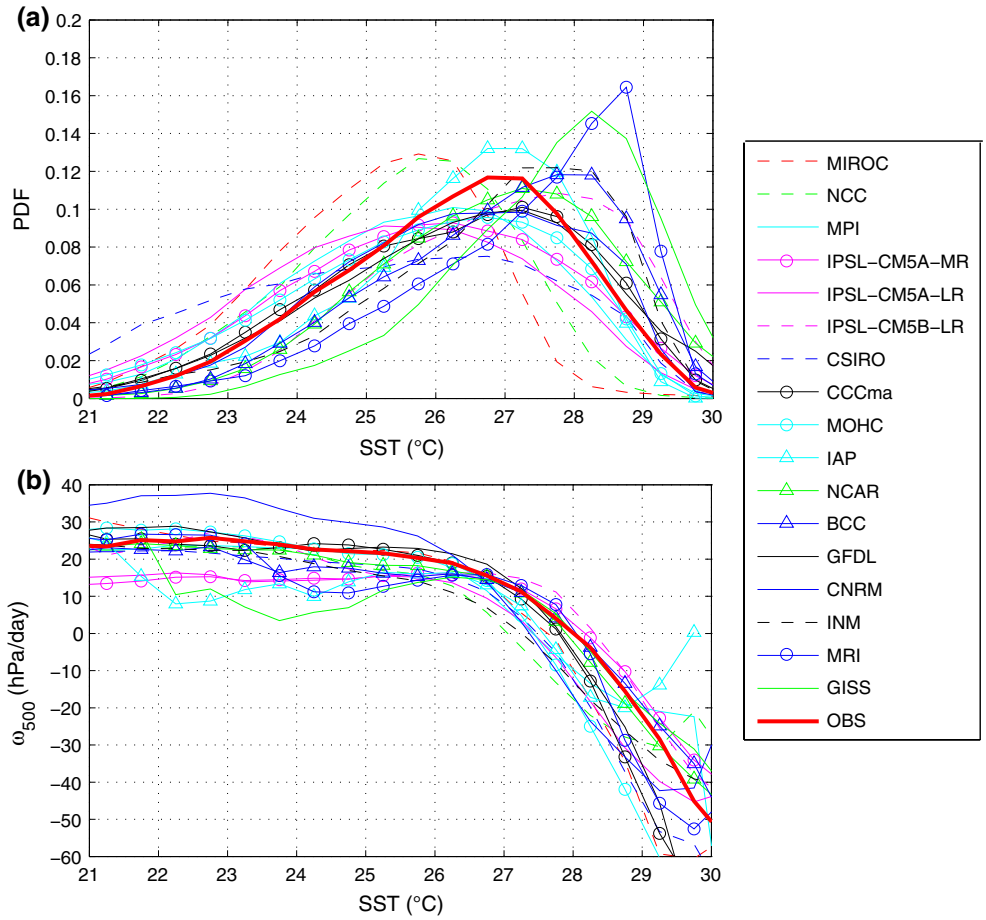

Fig. 6 **a** PDF of SST within 20°S–0°, 150°–100°W, **b** large-scale vertical velocity at 500 hPa ω_{500} as a function of SSTs within 20°S–0°, 150°–100°W for CMIP5 OAGCMs

cold-biased at monthly time-scale. MLT differs from the mean temperature because the shape of the PDF exhibits some significant inter-model differences. The average ω_{500} is computed for each 0.5 C SST bin over the DI region (see Fig. 6b). An SST threshold (THR) corresponding to the SST at which the mid-tropospheric vertical motion averaged over a given SST bin changes sign is identified as the SST threshold leading to the onset of deep convection.

The difference THR-MLT between SST threshold (THR) and the most likely SST over the DI region (MLT) is used to quantify the combined error of SSTs and local convection-SST coupling. This index measures the model likelihood to generate convection in the DI region by determining whether the ocean thermal conditions are more likely to lie beyond or below the model SST threshold for ascent (and sustained deep convection). Positive (negative) values of THR-MLT correspond to models whose most frequent thermal conditions in the southeastern tropical Pacific are colder (warmer) than the deep convection threshold, therefore producing a less (more) pronounced double ITCZ (Bellucci et al. 2010). The comparison between THR and MLT is relevant because it provides a combined information on both SST and convection triggering over the DI region. Indeed, anomalously warm surface temperatures in a model does not necessarily favor the onset of deep convection unless the SST threshold lies below the surface temperature.

4.2 The THR-MLT index in CMIP5 models: comparison with CMIP3 models

Figure 6 shows SST PDFs (Fig. 6a) and regime-sorted ω_{500} (Fig. 6b) for the CMIP5 OAGCMs. Similarly to CMIP3 models, most CMIP5 models exhibit lower THRs than the observed value (28 °C). However, the THR spread between CMIP5 models is smaller, within the 27–28.5 °C range (see Fig. 6b) compared to the 26–28.5 °C range found for CMIP3 models (Bellucci et al. 2010). The reduction of the spread is due to the improvement of three models: INMCM4, CNRM-CM5 and MIROC5, in which the THR has improved (27.5 °C instead of 26.5 °C in CMIP3 version). In particular, the more stringent threshold in MIROC5

might be explained by a modification in the parameterization of convective entrainment that tends to supress deep convection over dry, subsiding regions: Chikira and Sugiyama (2010) used an entrainment rate that depends on the buoyancy of the convective parcel, whereas the entrainment rate was previously uniform on the vertical.

The model SST shows a variety of distributions (see Fig. 6a). In particular, IAP-FGOALS-g2 produces an SST distribution in better agreement with the observations than in its CMIP3 version. This is likely to result from improvements in the LASG/IAP Climate system Ocean Model (LICOM2), in the representation of some physical processes such as the vertical turbulent mixing, the solar radiation penetration and the mesoscale eddy parametrization as well as in the advection scheme (Liu et al. 2012).

The strong relationship between the THR-MLT index and the double ITCZ error, established in CMIP3 models (Bellucci et al. 2010), is also verified in CMIP5 models (see Fig. 7), with positive THR-MLT corresponding to low double ITCZ error (e.g., MIROC5, NCC-NorESM1-M, IPSL-CM5A-MR) and negative THR-MLT corresponding to strong double ITCZ error (e.g., INMCM4, GISS-E2-R, MRI-CGCM3). The two indices' correlation is −0.89, similar to the CMIP3 value of −0.84. These results show the relevance of THR-MLT to study the SI spread between models. Indeed, we tried to test the strength of the relationship between SI and MLT or SI and the mean SST over the DI region and found that the correlations were not as strong (0.82 for the former and 0.64 for the latter). The anomalously strong precipitation over the DI region does not only depend on warm surface temperatures in that region but also on model SST threshold leading to the onset of convection.

This linear relationship can be written as a simple regression between the measured variable (SI) and the explanatory variable (THR-MLT) as follows:

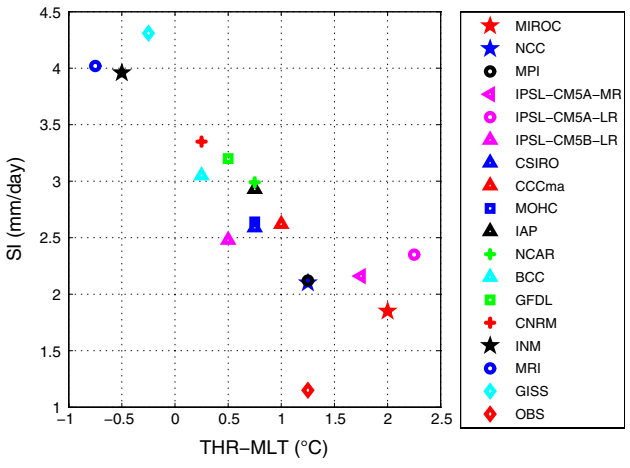

Fig. 7 Scatterplot of THR-MLT and SI index for CMIP5 OAGCMs and observations

Table 2 Results of the regression of the SI on THR-MLT (Eq. 1)

Eq. 1	α_1	p value	ϵ_0	$\overline{R^2}$
AMIP	−0.82	1×10^{-3}	0.86	0.5
CMIP	−0.83	1×10^{-5}	1.3	0.7

$$SI = \alpha_0 + \alpha_1 \, (THR - MLT) + \epsilon, \tag{1}$$

where $\alpha_0 = SI_{OBS} - \alpha_1 (THR - MLT)_{OBS} + \epsilon_0$ is the intercept, $\alpha_1 = -0.78$ mm day^{-1} °C^{-1} is the regression coefficient and ϵ is the residual. α_1 is statistically significant with a p value smaller than 10^{-4} using Student's statistical test. The observed value is $SI_{OBS} - \alpha_1 (THR - MLT)_{OBS} = 2.1$ mm day^{-1} and $\epsilon_0 = 1.3$ mm day^{-1} is the residual systematic error that is not accounted for by the error on THR-MLT. The regression results are summarized in Table 2.

To measure the goodness of fit of the statistical model defined by Eq. (1) (i.e. how well the regression line fits the set of data), we look at the adjusted R^2 ($\overline{R^2}$),[1] that is estimated at 0.7 for CMIP5 AOGCMs.

The strong relationship between the SI and the THR-MLT points out the importance of the thermodynamic forcing on precipitation in the DI region. This forcing is largely determined by local thermodynamic instability associated with warm SST and characterizes the local impact of SST on precipitation and the associated coupled ocean–atmosphere feedbacks. Figure 8 shows that the intermodel spread of THR-MLT is mostly due to that of MLT, and that the inter-model spread of THR has been reduced between CMIP3 and CMIP5 models (see also Fig. 6b); this suggests some convergence of the behaviours of AGCMs in terms of convection triggering. However, OAGCMs still present a wide spectrum of SST distributions due to the various configurations of ocean models and the variety of coupled feedbacks. These results explain the enhanced inter-model spread in SI index in the coupled ocean–atmosphere simulations compared to the AMIP simulations (see Fig. 3).

The relevance of THR-MLT highlights the local SST control on precipitation in CMIP5 models. However, it does not explain entirely the double ITCZ bias: the residual systematic error ϵ_0 is significant. Also, since this index is mostly controlled by MLT, which is imposed in AMIP simulations, we can wonder whether this index can explain the spread in SI index in AMIP simulations. This will be

[1] The coefficient of determination R^2 is the proportion of variability in a data set that is accounted for by the statistical model. It is defined as: $R^2 = \frac{\sum_i (\hat{SI}_i - \bar{SI}_i)^2}{\sum_i (SI_i - \bar{SI}_i)^2} = 1 - \frac{\sum_i (SI_i - \hat{SI}_i)^2}{\sum_i (SI_i - \bar{SI}_i)^2}$, where SI is the observed value, $\hat{SI}$ is the predicted value by the regression model and $\bar{SI} = \frac{1}{n} \sum_i SI_i$. $\overline{R^2}$ is the proportion of variability in a data set that is accounted for by the statistical model, that accounts for the number of explanatory variables in the model. It is defined as: $\overline{R^2} = 1 - \frac{n-1}{n-p} \frac{\sum_i (SI_i - \hat{SI}_i)^2}{\sum_i (SI_i - \bar{SI}_i)^2}$.

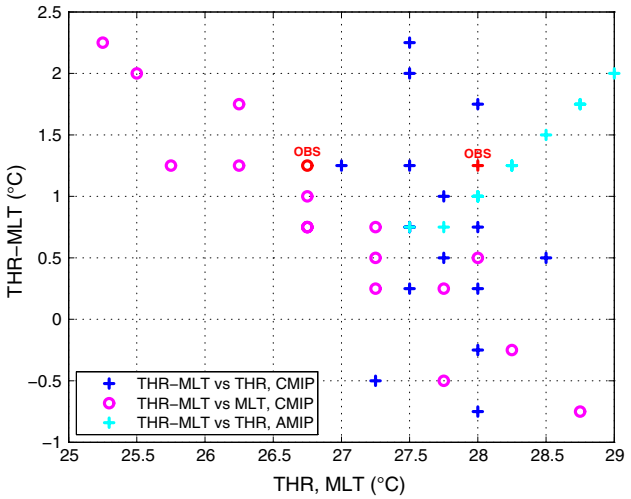

Fig. 8 Scatterplot of THR-MLT and (THR, MLT) for observations, CMIP5 OAGCMs and AGCMs

investigated in Sect. 4.3. Finally, some models with the same THR-MLT index, have different SI indices (see Fig. 7, e.g., IPSL-CM5B-LR and GFDL-ESM2M); it would be interesting to identify the mechanisms responsible for this spread.

4.3 The THR-MLT index in CMIP5 AGCMs

In this section, we apply the same regime analysis on the available CMIP5 AGCMs to investigate whether the relationship between the SI and THR-MLT indices holds also in these models.

AMIP simulations are performed using observed SSTs as a lower boundary condition for the atmospheric model. All the models have, therefore, the same most likely thermal state MLT (see Fig. 9a; a small difference in MLT can arise from the differing horizontal grids). The SST threshold THR for deep convection is still model-dependent. Vertical motions respond differently to imposed SST, resulting in a wide range of THR (see Fig. 9b). THR-MLT is directly controlled by THR, in contrast with the CMIP simulations in which it is strongly determined by MLT (see Fig. 8). The imposed oceanic conditions result in warmer THRs than in CMIP simulations and even than the observed THR for the majority of models (see Fig. 9b). This suggests that ocean–atmosphere coupling has a positive feedback on convection, resulting in an easier onset of convection and a less constrained SST threshold in CMIP simulations (see Fig. 6b).

Figure 10 shows the relationship between the SI index and THR-MLT in AMIP simulations. The linear relationship between these two indices is not as strong as in OAGCMs (SI and THR-MLT are correlated at the -0.76 level and $\overline{R^2}$ is 0.5). But it is still significant: when the linear regression between SI and THR-MLT, described by Eq. (1), is performed for AGCMs, α_1 is statistically significant (the p value of the corresponding statistical test is about 10^{-3}). Its estimate is -0.82 mm day^{-1} C^{-1}, similar to the estimation obtained for CMIP simulations. $\epsilon_0 = 0.86$ mm day^{-1} is the residual systematic error that is not accounted for by the error on THR-MLT. The regression results are summarized in Table 2.

This regression shows that, even in the absence of coupled feedbacks, the THR-MLT index still contains some information on the SI index. This information results from the atmospheric mechanisms controlling THR among which feedbacks between precipitation and vertical motion play a prominent role. Still, it is clear that the relationship between SI and THR-MLT is not as strong in the AGCMs as in OAGCMS, and that this relationship OAGCMs relies a lot on coupled mechanisms. In the next section, we attempt to introduce a more complete measure of the error on the relationship between dynamics and precipitation in the tropics that characterizes the model physics and relate it to the SI index.

5 Large-scale atmospheric contribution to the double ITCZ

5.1 Large-scale dynamics control on precipitation

Large-scale circulation and precipitation interact strongly in the tropical atmosphere. On one hand, large-scale ascent is associated with moisture convergence and upward transport, both favorable for convection. On the other hand, mid-level large-scale subsidence, and sometimes horizontal advection, can suppress convection through the drying effect on the atmospheric boundary layer, that reduces its moist static energy (Lau et al. 1997; Xie et al. 2010), and on the free troposphere, that can damp the convective plumes through entrainment (Chikira 2010; Hirota et al. 2011; Oueslati and Bellon 2013b). Deep convection, in turn, modifies the temperature gradients through latent heat release in cumulus clouds (e.g., Gill 1980) and convective cooling (Oueslati and Bellon 2013a); the resulting pressure gradients force the large-scale circulation. The interaction between dynamics and convection is, therefore, at the heart of the atmospheric mechanisms that control the tropical precipitation patterns.

Many observational studies have documented the relationship between precipitation and large-scale dynamics. Analysing the relationship between OLR (outgoing longwave radiation as a measure of convection) and SST, Lau et al. (1997) showed that the sensitivity of convection to local SST is strongly enhanced under strong large-scale upward motion within the 26–28 °C SST range. Above 28 °C, the intensity of convection is no longer dependent

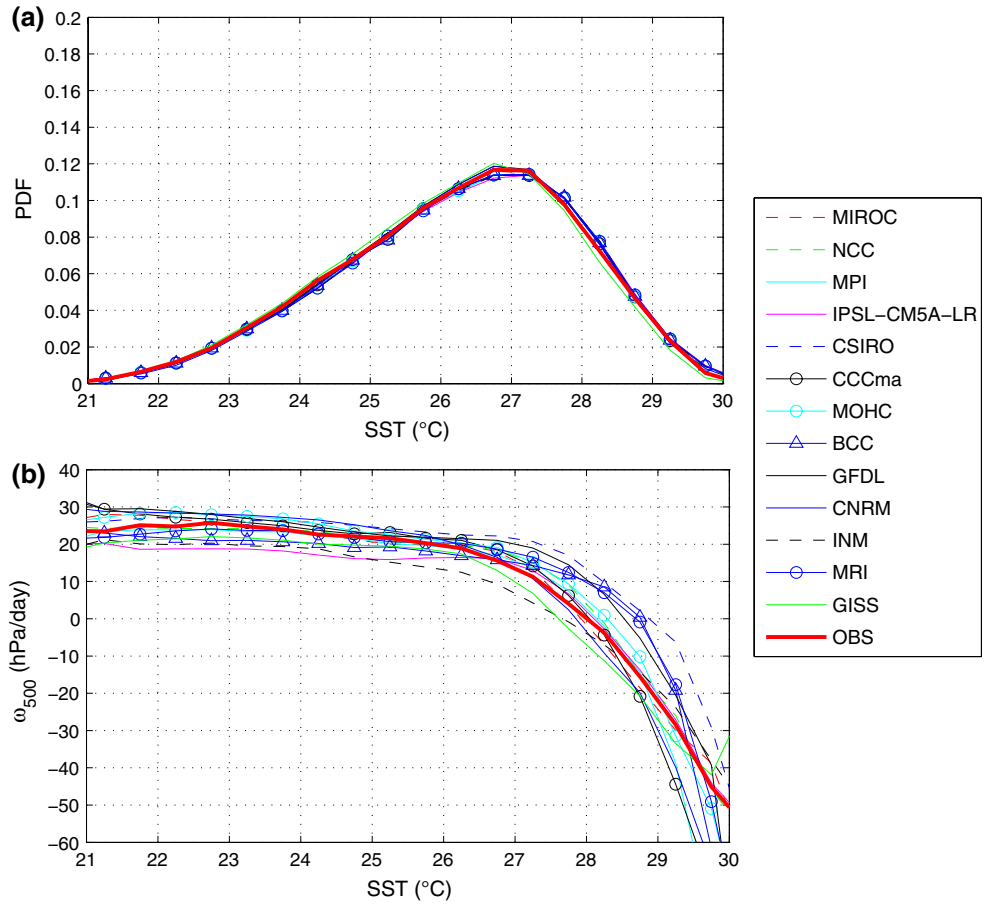

Fig. 9 **a** PDF of SST within 20°S–0°, 150°–100°W, **b** large-scale vertical velocity at 500 hPa ω_{500} as a function of SST within 20°S–0°, 150°–100°W for observations and CMIP5 AGCMs

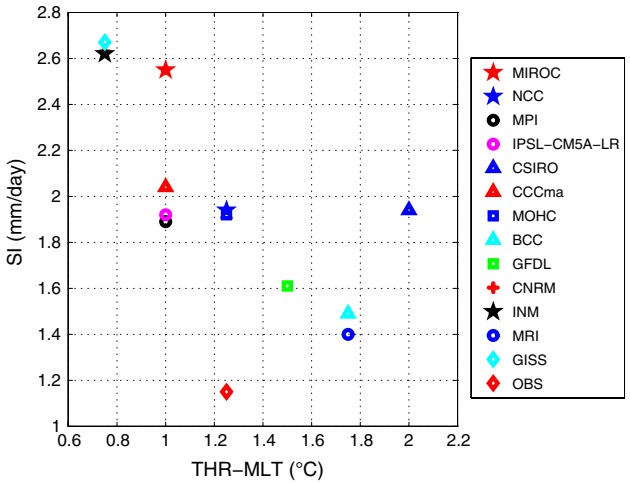

Fig. 10 Scatterplot of THR-MLT and SI index for CMIP5 AGCMs and observations

on the local SSTs, but it is more strongly controlled by the large-scale convergence (Graham and Barnet 1987; Gutzler and Wood 1990). In particular, a reduction in convection is observed in high SST "hot spot" situations which is likely to be explained by large-scale subsidence forced by nearby or remote deep convection (Lau et al. 1997).

The sensitivity of convection to large-scale circulation is not well represented in GCMs. In fact, in the CMIP3 models the precipitation patterns follow the SST patterns too closely compared to observations, especially over the southeastern tropical Pacific (Lin 2007). Hirota et al. (2011) argued that precipitation in models that overestimate precipitation in subsidence regions (e.g., the DI region) correlates strongly with SST and weakly with the large-scale circulation as diagnosed by ω_{500}. The physical processes suppressing convection, that convey the influence of subsidence are still poorly represented in OAGCMs. In particular, the more realistic distribution of precipitation observed in both MIROC5 and NCAR-CCSM4 is attributed to a stronger circulation-precipitation interaction, resulting from modifications of the convection schemes, that take into account the large-scale processes in the calculation of entrainment (in the case of MIROC5, Hirota et al.

2011) and CAPE-based closure (in the case of NCAR-CCSM4, Song and Zhang 2009).

Performing sensitivity studies with CNRM-CM5, Oueslati and Bellon (2013b) showed that the double ITCZ is associated with errors in the PDF of ω_{500} and the errors on the contribution of each ω_{500} regime to the total precipitation.

On the basis of this and the aforementioned studies, we introduce a measure of the errors in this contribution as a measure of the error in the precipitation-circulation relationship. We attempt to build a metrics defined globally (30°S–30°N) that measures a model's bias in simulating the interaction between circulation and precipitation. It characterizes the model physical parameterizations rather than the regional conditions in the DI region.

5.2 Combined precipitation circulation error (CPCE) and the double ITCZ bias

To study the precipitation-large-scale circulation coupling and its role in the double ITCZ bias, we use the sorting methodology of Bony et al. (2004) in which the monthly-mean mid-tropospheric (500 hPa) vertical pressure velocity ω_{500} is used as a proxy for large-scale ascent ($\omega_{500} < 0$) or subsidence ($\omega_{500} > 0$). The columns of the tropical atmosphere over oceans (30°S–30°N) are sorted into 10hPa bins of ω_{500}. The resulting PDFs of ω_{500} are shown in Fig. 11a for ERA40 and for CMIP5 AGCMs. We also compute the average precipitation for each ω_{500} regime in the observations (GPCP) and in AGCMs (see Fig. 11b). The contribution of each vertical regime to the total tropical precipitation is then quantified by weighting the regime-sorted precipitation by the PDF of ω_{500}. It is obtained by multiplying the PDF by the average precipitation for each ω_{500} bin (Bellucci et al. 2010). The resulting weighted precipitation distributions are shown in Fig. 11c.

The CMIP5 AGCMs simulate a PDF of ω_{500} similar to the observed distribution in the tropics, with a dominance of subsidence regimes (see Fig. 11a). Most models actually overestimate the maximum of occurrence of weakly subsiding regimes. The remaining models (CNRM-CM5 and INMCM4) overestimate the weakly ascending regimes, with hints of bimodality as documented in Oueslati and Bellon (2013b). In that study, a bimodal PDF of ω_{500} was attributed to feedbacks between large-scale circulation and deep convection that yield a strong double ITCZ bias. The models overestimate precipitation in all vertical regimes, particularly so in the ascending regimes (see Fig. 11b). This overestimation is even stronger in strong ascending regimes which explains, in particular, the excessive precipitation over the Maritime Continent, Indian Ocean, and within the Pacific ITCZ (see Fig. 1). The largest contribution to observed precipitation in the tropics derives from weak-to-moderate ascent and weak subsidence, with a maximum for ω_{500} in the -30 to -10 hPa day^{-1} range (see Fig. 11c). The majority of CMIP5 AGCMs capture the observed dominance of precipitation in weak-to-moderate ascent and weak subsidence. However, most of them overestimate the contribution of these particular regimes to precipitation (e.g., INMCM4, CNRM-CM5, IPSL-CM5A-LR...). In particular, biases in precipitation and regime frequency in weakly subsiding regimes may result from the misrepresentation of the different precipitation regimes associated with either occasional deep convection, mid-level convection associated with congestus, or shallow convection with precipitating cumuli. This can not be easily investigated because the precipitation data does not provide a partitioning between the different precipitation regimes, for either the global observations or the models.

As a metrics of a model's bias in simulating the interaction between circulation and precipitation, we propose to use the CPCE (Combined Precipitation Circulation Error) index which represents the quadratic error on the contribution of each vertical regime to the total precipitation over the tropical oceans. It is computed as the normalized quadratic error of the weighted precipitation shown in Fig. 11c. The quadratic calculation makes the CPCE more than a simple measure of precipitation by stressing the influence of each dynamical regime. It is weakly correlated to the tropical mean precipitation (coefficient of 0.3). CPCE is a global measure of the improper modelling of the circulation-precipitation coupling. It combines a measure of how poorly the models represent the distribution of dynamical regimes and how poorly the models simulate precipitation in a given dynamical regime. It characterizes therefore the model physics rather than the regional characteristics of the eastern Pacific.

CPCE is defined as follows:

$$CPCE = \frac{\sqrt{\sum_{-80\leq\omega\leq80}(\Delta(PDF_{\omega} \times P_{\omega}))^2}}{\sum_{-80\leq\omega\leq80}(PDF_{obs} \times P_{obs})} \quad (2)$$

where ω is the monthly-mean mid-tropospheric (500 hPa) vertical pressure velocity ω_{500}, PDF_{ω} is the PDF of ω_{500}, P_{ω} is the average precipitation for each ω_{500} regime, P_{obs} and PDF_{obs} are the observed distributions and Δ is the difference between the model and the observed distributions.

The purpose of the CPCE index is to quantify the errors in representing the interaction between precipitation and large-scale circulation in the tropics in order to understand their influence on precipitation biases in the DI region. To do so, the CPCE index should account for the large-scale properties of the DI region. In fact, one important difference between the distribution of vertical speed over the tropical belt and that in the DI region is the rare occurrence of strong ascending regimes ($\omega_{500} < -80$ hPa day^{-1}),

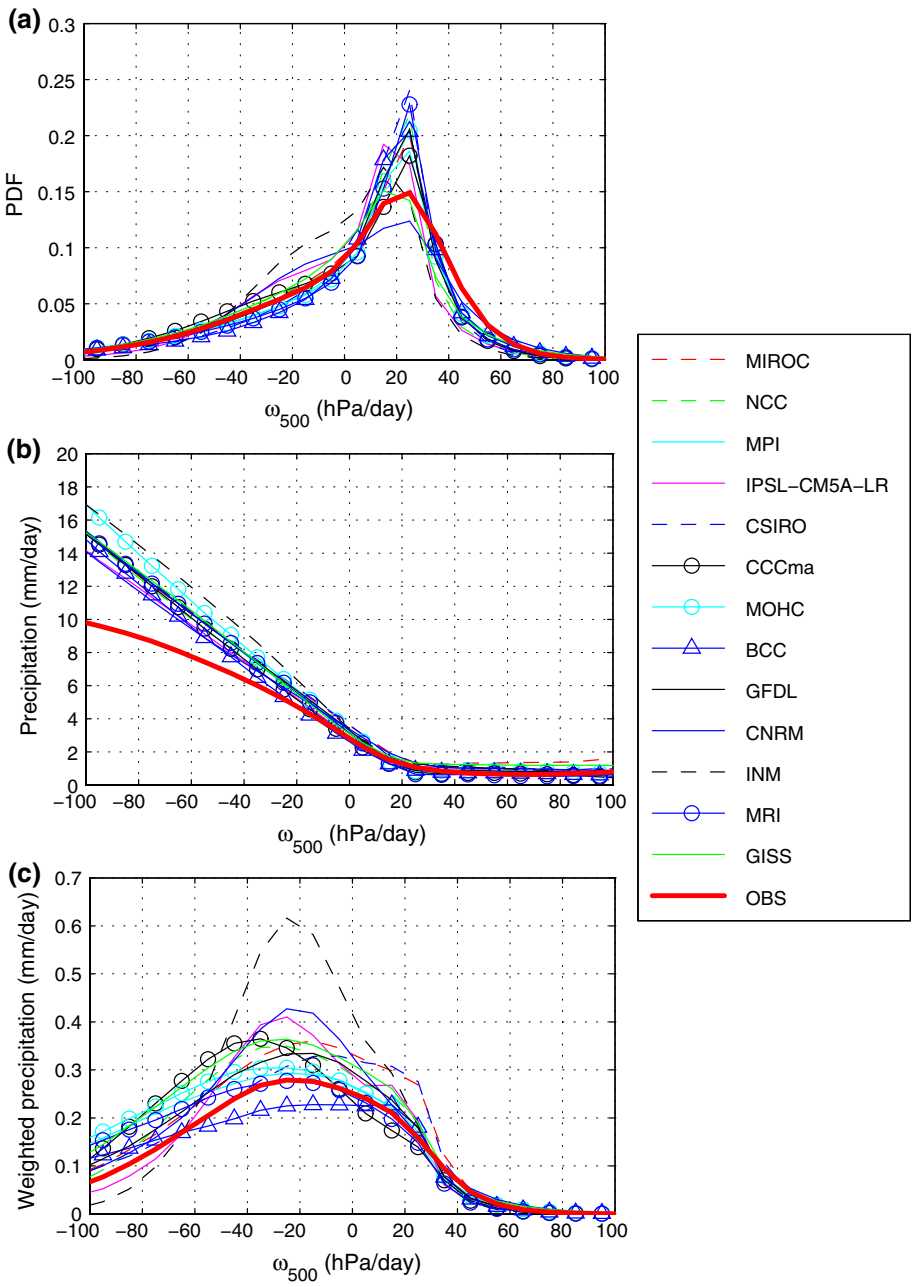

Fig. 11 **a** PDF of the 500 hPa large-scale vertical velocity ω_{500} in the tropics (30°S–30°N), **b** precipitation as a function of ω_{500}, **c** contribution to the mean tropical precipitation as a function of ω_{500}, derived from observations and CMIP5 AGCMs

with a frequency of occurrence close to zero, in the latter. Strongly ascending motions occur mostly within large regions of deep convection such as the warm pool and monsoon region. Precipitation biases in these regimes can be very large and hence have a strong impact on the CPCE, but that is not relevant for the bias we are studying. Based on this observation, the CPCE is computed for ω_{500} regimes between −80 and 80 hPa day^{-1}, accounting, therefore, for regimes that are important in the DI region and significant for the double ITCZ error. Indeed, we tried to relax this constrain and found that the results presented hereafter were not as clear, due to the additional error and inter-model spread arising from the strongly ascending regimes that are not relevant to the DI bias. Because they are infrequently observed, parametrized convection in these regimes is poorly constrained, resulting in large biases and inter-model spread.

The relationship between the CPCE index and the double ITCZ error in AGCMs is shown in Fig. 12. It appears that INMCM4 presents the largest CPCE index and is considerably distant from the rest of the models. A careful analysis of residuals, leverage and Cook's distance of the regression presented in the "Appendix" objectively shows that INMCM4 is an outlier. Geoffroy et al. (2012)

also diagnosed the anomalous character of INMCM4 when analysing the global thermal properties of CMIP5 models. Thus, it seems reasonable to exclude INMCM4 in the following analyses.

A strong linear relationship between the CPCE and SI indices can be seen in Fig. 12 and the correlation between the two is 0.85 (slightly larger than the correlation between the SI and THR-MLT). The linear regression between the SI and the CPCE in AGCMs can be written as:

$$SI = \alpha_0 + \alpha_2\, CPCE + \epsilon, \tag{3}$$

where $\alpha_0 = SI_{obs} + \epsilon_0$, with $\epsilon_0 = -0.25$ mm day^{-1} and $\alpha_2 = 14.6$ mm day^{-1}. α_2 is statistically significant (the p value of the corresponding statistical test is smaller than 10^{-3}). The regression results are summarized in Table 3.

The linear regressions described by Eqs. (1) and (3) show that in AGCMs, both THR-MLT and the CPCE can explain the spread in SI. Since AGCMs have the same SST forcing, both indices are measures of the interaction between dynamics and precipitation. They are highly correlated (coefficient of 0.7) and therefore carry overlaping information. However, comparing $\overline{R^2}$ between the two regression models, we can see that $\overline{R^2}$ in the regression model defined by Eq. (3) is higher than that defined by Eq. (1) ($\overline{R^2} = 0.7$ instead of 0.5). Also, the unexplained bias in the regression defined by Eq. (3) is smaller than the unexplained bias in the regression defined by Eq. (1) ($\epsilon_0 = -0.25$ mm day^{-1} instead of 0.86 mm day^{-1}). Therefore, the SI bias and spread in CMIP5 AGCMs are better explained by CPCE than by THR.

To further clarify the relative roles contributed by large-scale dynamics (CPCE) and local SST (THR-MLT) on the double ITCZ bias (SI) in AGCMs and OAGCMs, the next section is dedicated to a regression analysis on both predictors.

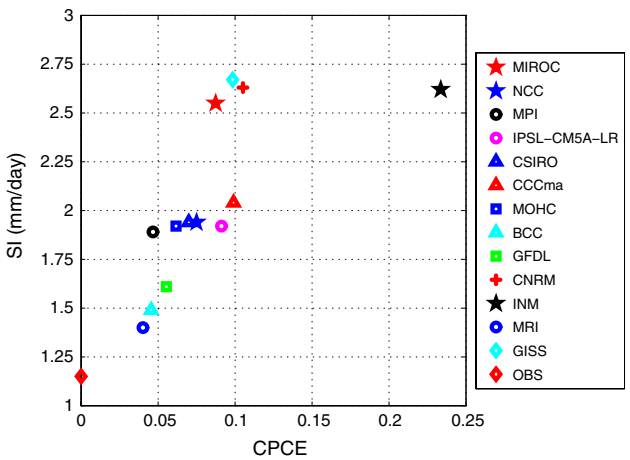

Fig. 12 Scatterplot of CPCE and SI index for CMIP5 AGCMs and observations

Table 3 Results of the regression of the SI on the CPCE (Eq. 3)

Eq. 3	α_2	p value	ϵ_0	$\overline{R^2}$
AMIP	14.6	5×10^{-4}	−0.25	0.7

6 Respective roles of SST and circulation-precipitation interaction in the double ITCZ bias

The interaction between SST, large-scale dynamics and precipitation is examined by performing a multiple linear regression of the SI on both THR-MLT and CPCE in a manner similar to Bellon et al. (2010):

$$SI = \alpha_0 + \alpha_1\, (THR - MLT) + \alpha_2\, CPCE + \epsilon, \tag{4}$$

where $\alpha_0 = SI_{OBS} - \alpha_1 (THR - MLT)_{OBS} + \epsilon_0$ is the intercept, α_1 and α_2 are regression coefficients and ϵ is the residual.

The statistical significance of the coefficients α_1 and α_2 is checked by Student's statistical test of the null hypothesis H_0 against an alternative hypothesis H_1 defined as:

H_0 : $\alpha_i = 0$ (α_j being estimated);

H_1 : $\alpha_i \neq 0$ (α_j being estimated);

with (i, j) = (1, 2) or (2, 1).

The results of the regression are summarized in Table 4.

6.1 AGCMs

The regression of the SI index is performed for AGCMs. Only α_2 is statistically significant at the 98 % confidence level (the p value associated to the statistical test is 0.02). The p value on the regression coefficient for THR-MLT is higher than 0.05. The null hypothesis for α_1 is therefore accepted and the regression model proposed by Eq. (4) reduces to the one of Eq. (3). This shows that CPCE provides a more complete information on the AGCM error on the SI than the threshold THR, and that the information provided by THR is actually comprised in the CPCE.

Table 4 Results of the regression of the SI on THR-MLT and the CPCE (Eq. 4)

Eq. 4	α_1	p value	α_2	p value	ϵ_0	$\overline{R^2}$
CMIP	−0.77	7×10^{-7}	7.3	5×10^{-3}	0.7	0.85

6.2 OAGCMs

6.2.1 The CPCE index in OAGCMs

In AGCMs, dynamics-precipitation interaction is the driver of the double ITCZ bias. Given that THR-MLT failed to explain entirely the double ITCZ bias in OAGCMs, it seems interesting to investigate the role of the large-scale atmospheric processes and see whether the CPCE provides additional information on the SI index in OAGCMs.

The ω_{500} regime-sorting approach is applied to CMIP5 simulations. The obtained distributions are shown in Fig. 13. OAGCMs produce the same characteristics as the corresponding AGCMs in ω_{500} regime frequency and precipitation magnitude for individual regimes (see Figs. 11, 13), with the exception of IAP-FGOALS-g2 that slightly underestimates precipitation in strong ascent and overestimates precipitation in weak subsidence. Indeed, alike AMIP simulations, CMIP ones overestimate the contribution of weak-to-moderate ascent and weak subsidence to the total tropical precipitation (e.g., INMCM4, GISS-E2-R, CNRM-CM5. . .). These similar characteristics between the two model configurations reveal that the misrepresentation of the precipitation/large-scale dynamics relationship is an intrinsic characteristic of the AGCMs essentially independent of coupled ocean–atmosphere feedbacks.

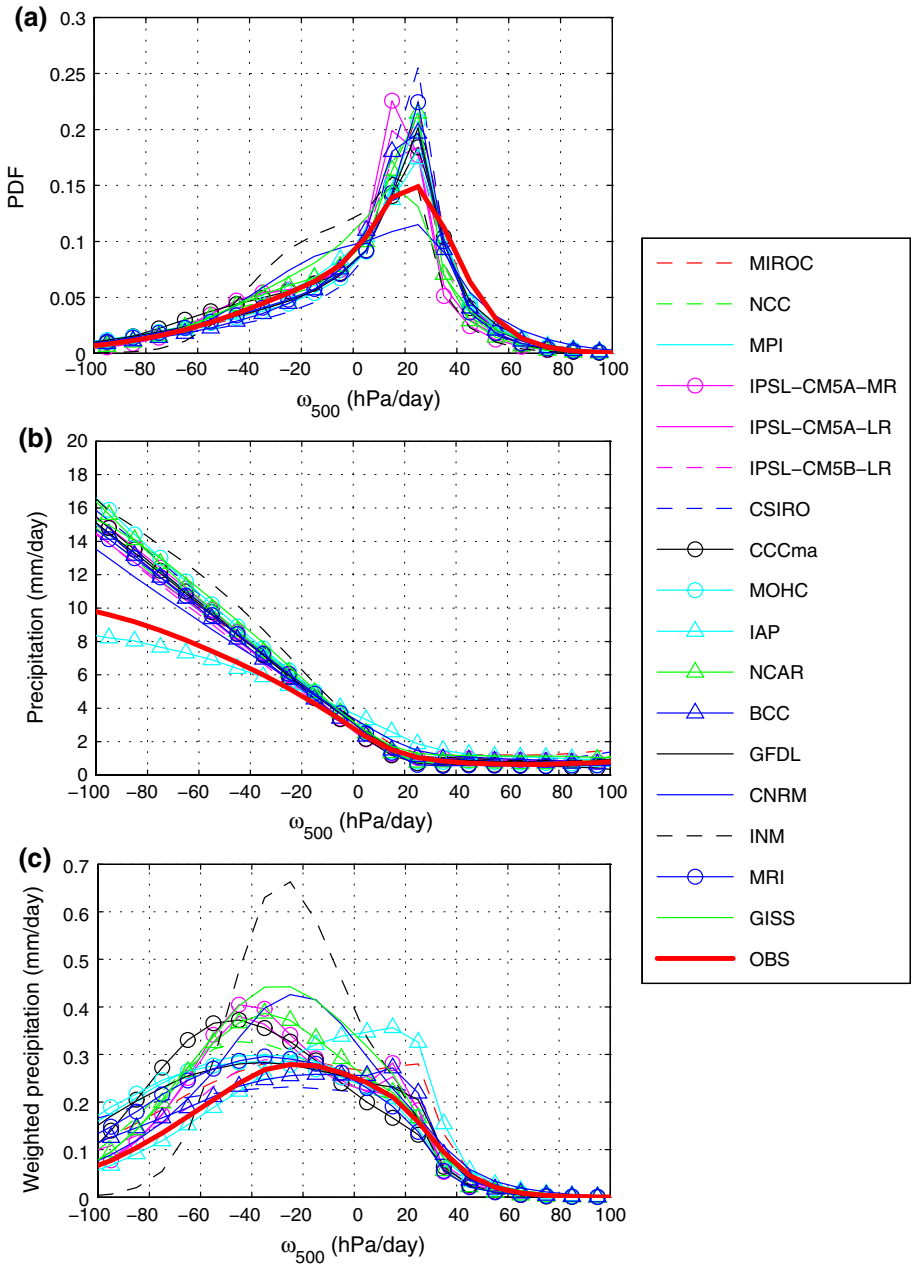

Fig. 13 **a** PDF of the 500 hPa large-scale vertical velocity ω_{500} in the tropics (30°S–30°N), **b** precipitation as a function of ω_{500}, **c** contribution to the mean tropical precipitation as a function of ω_{500}, derived from observations and CMIP5 OAGCMs

Based on the shape of the weighted precipitation distribution, the CMIP5 models can be gathered into three groups (Bellucci et al. 2010). The first collects the majority of models which capture the observed dominance of precipitation in weak-to-moderate ascent and weak subsidence. The second group collects models displaying two relative maxima, in both ascending and subsiding regimes (IPSL-CM5A-LR, IPSL-CM5A-MR, MIROC5 and CSIRO-Mk3-6-0). The third group corresponds to models which exhibit a maximum contribution to precipitation in subsiding regimes. This group only includes IAP-FGOALS-g2. Despite the erroneous maximum, IAP-FGOALS-g2 produces simulates a contribution of moderately and strongly ascending.

The role of dynamics-precipitation interaction on the double ITCZ in OAGCMs is examined by displaying the CPCE index as a function of the SI index (see Fig. 14). Again INMCM4 is identified as an outlier (see Fig. 18a in the "Appendix") and excluded from the following analyses. Unlike in the AMIP simulations, no obvious link appears between the CPCE and the SI in OAGCMs. The correlation between the CPCE and the SI is 0.3. By itself, the CPCE is unable to explain the inter-model spread of the double ITCZ bias in the CMIP simulations. But it is interesting to investigate whether the CPCE provides additional information to THR-MLT. The multiple linear regression of the SI on both THR-MLT and CPCE (described by Eq. 4) is thus performed.

In both cases, H_0 can be rejected at the 95 % confidence level. This shows that, in OAGCMs, THR-MLT and the CPCE provide independent and complementary information on the SI index. The coefficient α_1 is estimated to $-0.77\ \mathrm{mm\,day^{-1}}\ C^{-1}$ (with a p value of about 10^{-6}), a value similar to the regression on THR-MLT only (see Eq. 1); this shows that the CPCE and THR-MLT provide information that overlap very little (indeed, the correlation between THR-MLT and the CPCE is 0.03). The linear regression provides the following estimates: $\alpha_2 = 7.3\ \mathrm{mm\,day^{-1}}$ (with a p value of 5×10^{-3}), $\alpha_0 = 2.8\ \mathrm{mm\,day^{-1}}$ and $\epsilon_0 = 0.7\ \mathrm{mm\,day^{-1}}$.

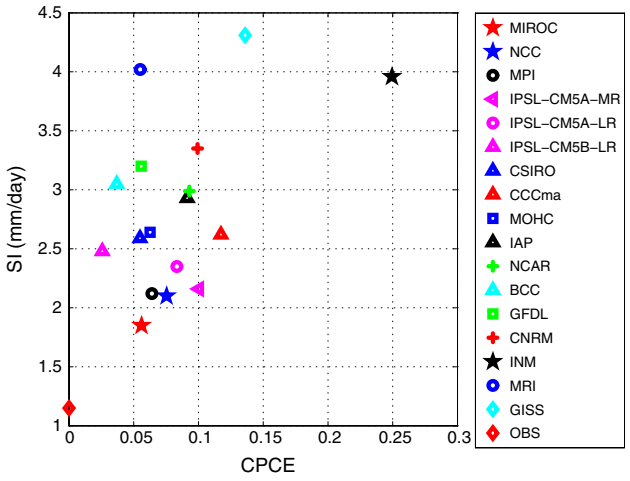

Fig. 14 Scatterplot of CPCE and SI index for CMIP5 OAGCMs and observations

The robustness of this regression model as well as the appropriateness of excluding INMCM4 is verified by checking each model residuals, leverage and Cook's distance (see Fig. 18 in the "Appendix").

The regression model in Eq. (4) provides a more complete set of drivers of the double ITCZ than the model of Eq. (1). This is illustrated by the increased adjusted R^2 ($\overline{R^2}$). $\overline{R^2} = 0.85$ in the regression model defined by Eq. (4) instead of 0.7 in that defined by Eq. (1). In addition, the unexplained bias is smaller than in Eq. (1) ($\epsilon_0 = 0.7\ \mathrm{mm\,day^{-1}}$ instead of $1.3\ \mathrm{mm\,day^{-1}}$), showing that a larger part of the error on the SI is better accounted for by the statistical model defined by Eq. (4). Physically, this multiple regression proves that even if the amplitude of the double ITCZ bias results mostly from a miss-representation of coupled atmosphere-ocean processes in OAGCMs, this bias is significantly modulated by errors in the simulation of the interaction between precipitation and circulation by the AGCMs. However, $\epsilon_0 \neq 0$ shows that the two metrics are insufficient to account for the entire double-ITCZ bias. Determining which mechanisms are not quantified by these metrics warrants further investigation.

Again we can investigate the added value of the CPCE as a measure of the circulation-precipitation interaction, compared to a simple precipitation mean in OAGCMs. To do so, we perform a multiple linear regression of the SI on both THR-MLT and mean precipitation and show that only the regression coefficient associated to THR-MLT is statistically significant (with a p value of 5×10^{-2}). Tropical precipitation mean does not provide any information independent from THR-MLT. By contrast, THR-MLT and CPCE provide independent and complementary information on the SI.

To summarize the different contributions to the SI bias in OAGCMs, we rewrite Eq. (4) to express the SI bias:

$$\Delta SI = \alpha_1\ \Delta(THR - MLT) + \alpha_2\ CPCE + \epsilon + \epsilon_0, \qquad (5)$$

where Δ indicates the difference between the model and the observed values. This decomposition of the SI bias in OAGCMs are shown in Fig. 15.

Models producing pronounced double ITCZ bias (e.g. GISS-E2-R, MRI-CGCM3, GFDL-ESM2M...) show significant and positive biases in representing both atmospheric and coupled processes. Combined, these biases result in a larger SI bias. In contrast, models producing a smaller SI bias (e.g. MIROC5, IPSL-CM5A-LR, IPSL-CM5A-MR) show a negative bias on THR-MLT, that compensates the

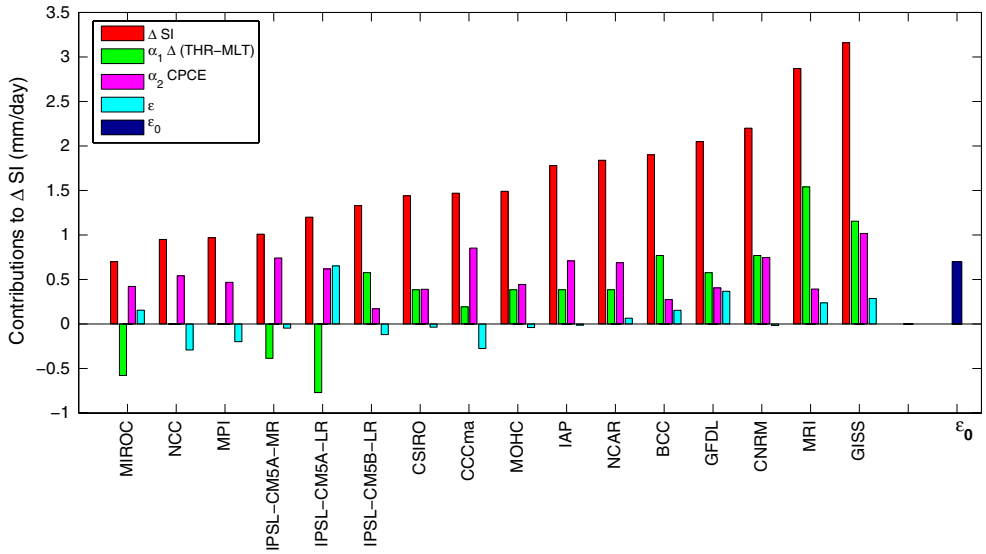

Fig. 15 Contribution of atmospheric and coupled processes biases to the SI bias in OAGCMs computed from Eq. (5)

error on the simulated relationship between circulation and convection. In these models, SST and associated coupled feedbacks described by THR-MLT compensate for the bias due to atmospheric processes. This, explains, in particular, the larger SI produced in the AMIP simulations of MIROC5 compared to the CMIP simulations. This is not the case in IPSL-CM5A-LR and IPSL-CM5A-MR, where the SI bias is amplified in CMIP simulations, which suggests that other coupled processes are misrepresented in OAGCMs that are not accounted for by the THR-MLT index. In addition, for models with small SI bias where biases in THR-MLT and CPCE compensate, only ϵ_0 remains. It may result from the misrepresentation of processes that are not considered in the CPCE and THR-MLT, such as the subgrid transport and turbulent surface fluxes or the influence of extratropics (Hwang and Frierson 2013). Overall, it appears that the misrepresentation of the interaction between convection and circulation (as measured by the CPCE) explains a significant fraction of the SI bias, but the misrepresentation of coupled processes (as measured by THR-MLT) explains most of the inter-model spread.

6.2.2 *Decomposition of the weighted precipitation bias in OAGCMs*

A more detailed description of the precipitation-large-scale circulation interaction can be obtained by decomposing the weighted precipitation bias in each CMIP5 model into three terms:

$$\Delta(PDF_\omega \times P_\omega) = \Delta PDF_\omega \times P_{obs} + \Delta P_\omega \times PDF_{obs} + \Delta PDF\omega \times \Delta P\omega \quad (6)$$

where PDF_ω is the ω_{500} PDF, P_ω is the average precipitation for each ω_{500} regime, P_{obs} and PDF_{obs} are the observed distributions and Δ indicates the difference between the model and the observed values. The first term corresponds to the bias in the PDF. It is associated with the circulation bias. The second term corresponds to the bias resulting from the biases of precipitation simulated in each dynamical regime, considered to be the thermodynamical contribution. The third term is associated with the covariation of dynamical and thermodynamical biases. The contributions to the weighted precipitation bias, ordered with ascending CPCE index, are shown in Fig. 16.

A common characteristic of all but one (the IAP-FGOALS-g2) models is their overestimation of the precipitation in the ascending regimes. This contributes significantly to the CPCE, but it contributes little to the inter-model spread since the models exhibit similar biases.

The model IPSL-CM5B-LR produces the lowest CPCE index (see Fig. 14) through error compensation between dynamical and thermodynamical biases in ascending and subsiding regimes.

A common characteristic between the other CMIP5 models appears within weak-to-moderate ascending regimes ($-60 < \omega_{500} < 0$ hPa day^{-1}): comparing the shape of the different distributions, it appears that the error on the weighted precipitation ($\Delta(PDF_\omega \times P_\omega)$) is controlled by the error in the frequency of occurrence of vertical regimes ($\Delta PDF_\omega \times P_{obs}$), rather than the error in precipitation intensity within each regime ($\Delta P_\omega \times PDF_{obs}$). This error on the PDF controls the inter-model spread: models with small CPCE (e.g., BCC-CSM1-1, CSIRO-Mk3-6-0...) tend to underestimate the frequency of

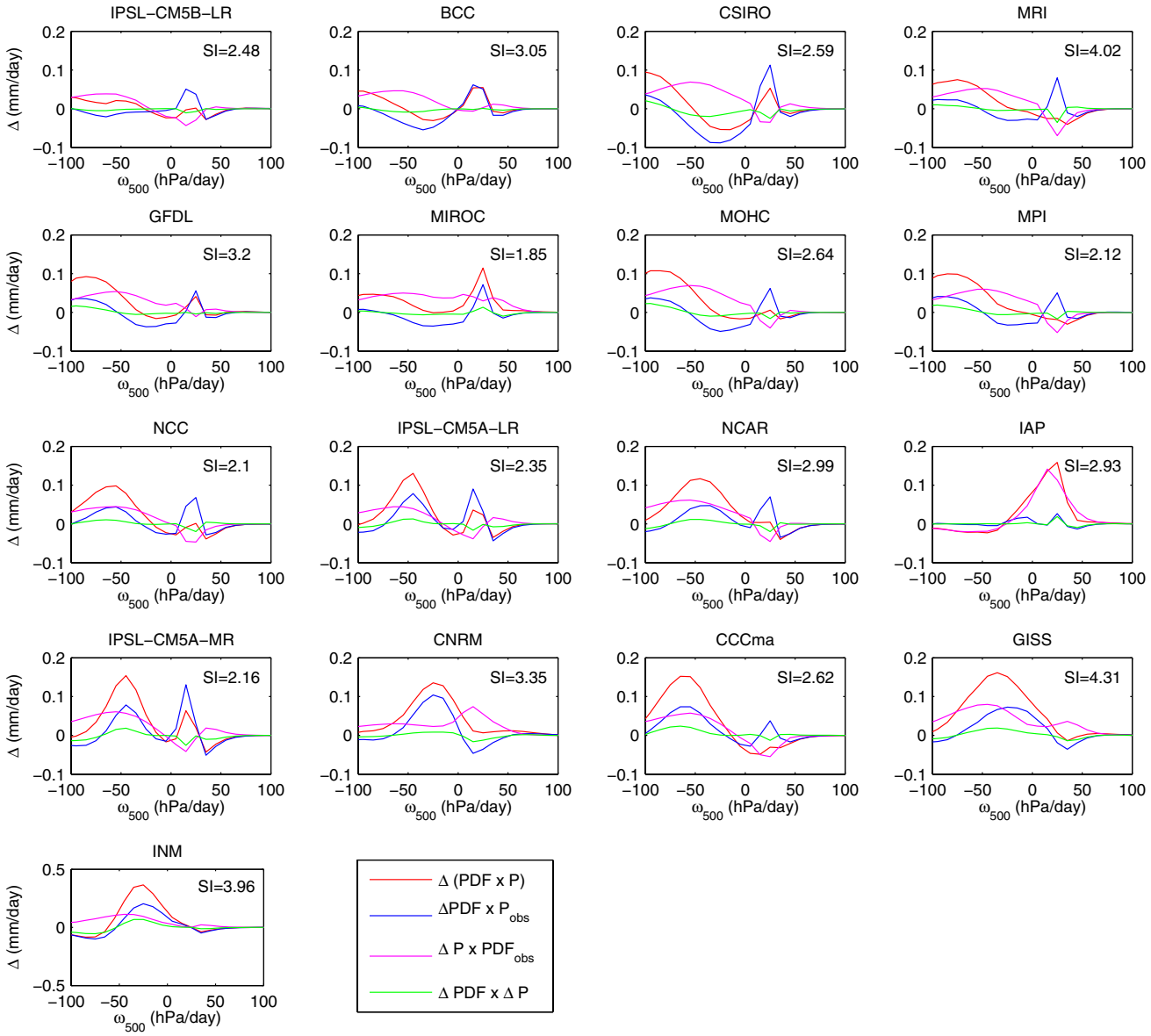

Fig. 16 Decomposition of the weighted precipitation bias into three contributions from the PDF bias, the precipitation intensity bias and the co-variation of dynamic and non-dynamic biases. The figure panels are ordered with ascending CPCE i.e. the first panel correspond to the model with the lowest CPCE

weak-to-moderate ascent that compensate the overestimation of the precipitation intensity, while models with larger CPCE index (e.g., CNRM-CM5, GISS-E2-R,...) overestimate both the precipitation intensity and the frequency of occurrence of weak-to-moderate ascending regimes. This combination of errors is pointed out in Oueslati and Bellon (2013b) as strongly associated with the double ITCZ bias.

Under strong ascending regimes ($\omega_{500} < -60\,\mathrm{hPa\,day^{-1}}$), the error in regime frequency is less important and it is the error in precipitation intensity that determines the amplitude of the weighted precipitation error. These regimes, however, play a minor role on the double ITCZ problem as already mentioned.

Two model behaviours can be distinguished regarding the contribution of subsiding regimes to the total precipitation. Models showing distributions close to observations result from a compensation between dynamical and thermodynamical errors (e.g., MOHC-HadGEM2-ES). The others present larger errors, which, with the exception of IAP-FGOALS-g2, are explained by dynamical errors (e.g., MIROC5).

To summarize, the inter-model spread in the CPCE is mostly due to the spread in the frequency of occurrence of vertical regimes, and the error in precipitation intensity within each regime contribute significantly to the CPCE for all models (Bellucci et al. 2010; Oueslati and Bellon 2013b). Errors in regime frequency are most often an overestimation of the frequency of both weak-to-moderate ascending regimes and subsiding regimes. However, only the error in weak-to-moderate ascending regimes is most likely to influence the double ITCZ error.

7 Summary and conclusions

This study examines the double ITCZ problem in CMIP5 (Coupled Model Intercomparison Project phase 5) OAGCMs and AGCMs. The monthly outputs of 21 years (1979–1999) of simulations from 17 OAGCMs are analysed, together with the 13 available AMIP simulations.

The results show that all the models still suffer from the double ITCZ bias to some extent, with a too-zonally elongated SPCZ and a spurious ITCZ in the Eastern Pacific. Since CMIP3, the simulation of the ITCZ has improved only in a few models, either through increased resolution (IPSL-CM5A, CNRM-CM5, MPI-ESM-LR) or improved convection parametrization (NCAR-CCSM4, IPSL-CM5B-LR). Comparing the Southern ITCZ (SI) index, it appears that the double ITCZ bias has become small in AMIP simulations, and that coupled atmosphere-ocean feedbacks still account for a large part of this bias in CMIP simulations, similarly to the previous generations of models (Lin 2007).

The present study tried to build a process-oriented metrics that captures the contribution from the interaction between large-scale circulation and deep convection to the double ITCZ bias and its intermodel spread, additionally to the well-documented role of the ocean–atmosphere feedbacks.

The role of SST and the associated coupled feedbacks is examined through the THR-MLT index (Bellucci et al. 2010). This index estimates the likelihood for a given model to yield deep convection in the DI region, combining biases on the representation of local most frequent SSTs (MLT) and the SST threshold leading to the onset of ascent (THR) in the DI region. The high correlation between THR-MLT and the SI found in CMIP3 models (Bellucci et al. 2010) is verified in the new generation of OAGCMs (with a correlation coefficient of −0.89), showing that the double ITCZ problem is mainly thermodynamically driven by the local SSTs in southeastern Pacific. However, performing a simple regression between the SI and THR-MLT, it appears that THR-MLT does not explain entirely the double ITCZ bias. In addition, since AMIP simulations have the same oceanic forcing, THR-MLT is directly controlled by THR, in contrast with OAGCMs where it is strongly determined by the model SST biases. Among the mechanisms controlling THR, feedbacks between precipitation and large-scale dynamics play a dominant role. Indeed, if the interaction between precipitation and large-scale ascent is sufficiently strong, the atmosphere can sustain precipitation and ascent with little surface turbulent fluxes.

The error on the interaction between precipitation and circulation can be measured by the Combined Precipitation Circulation Error (CPCE). This index is defined using the mid-tropospheric vertical velocity ω_{500} sorting methodology (Bony et al. 2004) in the tropics (30°S–30°N). It is computed as the quadratic error on the contribution of each vertical regime to the total precipitation over the tropical oceans. CPCE characterizes the model physics rather than the regional characteristics of the eastern Pacific. It combines biases in the frequency of occurrence of vertical regimes and in the rainfall magnitude associated with each individual regime. In AGCMs, the relationship between the SI and the CPCE is stronger than that between the SI and the THR-MLT, with a correlation coefficient of 0.87. This shows that the SI spread between AGCMs is better accounted for by the CPCE and points out the important role played by precipitation-large-scale dynamics interaction in the double ITCZ bias. The role of CPCE in coupled ocean–atmosphere simulations is investigated by performing a multiple linear regression of the SI on both THR-MLT and CPCE. This new regression model provides a significantly more complete description of the SI than a regression on THR-MLT alone. The precipitation bias in southeastern tropical Pacific is driven by biases on local thermodynamical coupled processes associated with SST and on the global characteristics of the dynamical mechanisms associated with the precipitation-circulation coupling. The coupled processes account in particular for the inter-model spread. In some models (MIROC5, IPSL-CM5A-LR, IPSL-CM5A-MR), coupled processes biases described by THR-MLT reduce the double ITCZ bias. It results, in the case of MIROC5, in a smaller SI bias in CMIP simulations compared to AMIP simulations.

The inter-model spread in simulating the precipitation-dynamics relationship is dominantly due to the spread in the frequency of occurrence of weak-to-moderate ascending regimes (Bellucci et al. 2010; Oueslati and Bellon 2013b). Overestimated ascending regimes suggest that processes inhibiting deep convection (e. g. convective entrainment, downdrafts and large-scale subsidence) are still poorly represented in CMIP5 models. A better representation of some observed negative feedbacks on convection

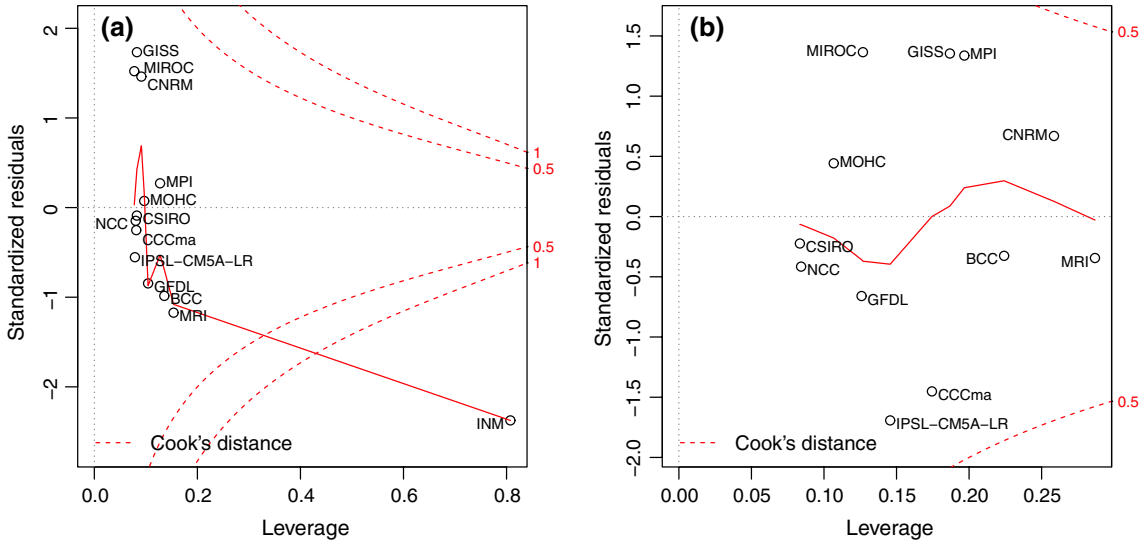

Fig. 17 Standardised residuals versus leverage plot of the linear regression described in Eq. (3), performed with atmoshpere-only models including (**a**) and excluding (**b**) INMCM4. The *red line* corresponds to the loess curve that fits to the scatter plot. *Contour lines* represent the Cook's distance

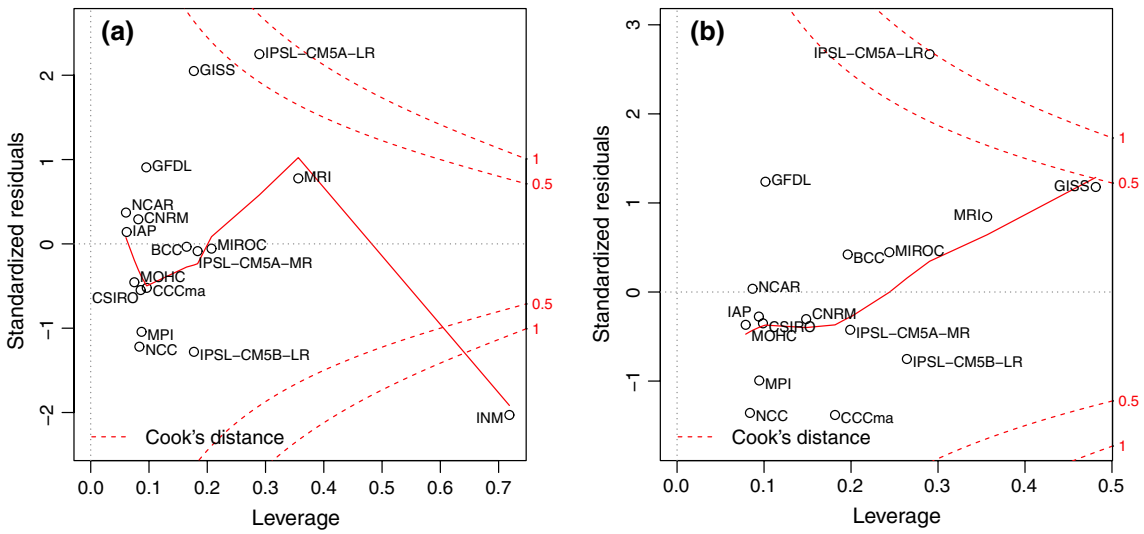

Fig. 18 Standardised residuals versus leverage plot of the regression model described in Eq. (3) including (**a**) and excluding (**b**) INMCM4. The *red line* corresponds to the loess curve that fits to the scatter plot. *Contour lines* represent the Cook's distance

can help alleviate the double ITCZ. In particular, in some models (e. g. IPSL-CM5A-LR, IPSL-CM5A-MR, NCC-NorESM1-M), the smaller double ITCZ bias is explained by an overestimated frequency of subsiding regimes, that tends to suppress deep convection through lower-tropospheric drying.

Our analysis suggests that the THR-MLT (Bellucci et al. 2010) and the CPCE indices are relevant metrics to quantify the biases on SST and large-scale dynamics in OAGCMs and AGCMs that affect the double ITCZ bias. But they fail to explain completely the bias on SI. More efforts toward the construction and the use of such metrics are needed to evaluate climate model performance.

Acknowledgments We would like to thank Aurélien Ribes for helpful discussions. We also acknowledge the World Climate Research Programme's Working Group on Coupled Modelling, which is responsible for CMIP, and we thank the climate modeling groups (listed in Table 1 of this paper) for producing and making available their model output. For CMIP the U.S. Department of Energy's Program for Climate Model Diagnosis and Intercomparison provides coordinating support and led development of software infrastructure in partnership with the Global Organization for Earth System Science Portals.

Appendix

Evaluating the results of a linear regression

To validate the results of a linear regression, it is important to examine the residuals (ϵ) from the regression and identify extreme data points (leverage), that can potentially exercise a great influence on the regression line. The residuals are normalized (i.e., divided by the standard deviation of the residuals) in order to make the analysis on a standard scale.

The leverage is based on how the observed values differ from the values predicted by the regression model: $\hat{SI} = H\ SI$, where SI is the vector of observed values, $\hat{SI}$ is the vector of values predicted by the regression model and H is the hat matrix. The leverage of the i-th value is the i-th diagonal element (h_{ii}) of the hat matrix H.

Combining both residuals and leverage, we obtain a measure of the actual influence each point has on the slope of the regression line, namely the Cook's distance. Cook's distance is a measure of the effect of deleting a given observation on the regression analysis (Cook and Weisberg 1982).

Cook's distance is calculated as: $D_i = \frac{\sum_{j=1}^{n}(\hat{SI}_j - \hat{SI}_{j(i)})^2}{p\ MSE}$, where $\hat{SI}_j$ is the prediction from the full regression model for observation j, $\hat{SI}_{j(i)}$ is the prediction for observation j from a refitted regression model in which observation i has been omitted, MSE is the mean square error of the regression model and p is the number of parameters in the model. Cook's distance can be expressed as a function of both residuals and leverage: $D_i = \frac{\epsilon_i^2}{p\ MSE}[\frac{h_{ii}}{(1-h_{ii})^2}]$, where ϵ_i is the residual of the regression. Data points with large residuals and/or high leverage may alter the result of the regression.

Smaller Cook's distances means that removing the observation has little effect on the regression results. Distances larger than 1 are suspicious and suggest the presence of a possible outlier or a poor model.

Figure 17 shows the standardised residuals versus leverage plot of the regression model, described by Eq. (3), performed with AGCMs, with and without INMCM4. The relationship between residuals and leverage is highlighted through a LOESS curve (LOcal regrESSion,[2] Fox 2002). Superimposed on the plot are contour lines for the Cooks distance.

Comparing the two plots, we see that the regression performed without INMCM4 (see Fig. 17b) exhibit smaller residuals and leverage. Indeed, the values of Cook's distance are inferior to 1. This confirms the robustness of the regression model described by Eq. (3) in AGCMs and validates the exclusion of INMCM4.

Figure 18 shows the same plot of the regression model, described by Eq. (4), performed with OAGCMs, with and without INMCM4. Again, INMCM4 is identified as an outlier (see Fig. 18a). Indeed, after excluding INMCM4, residuals and leverage are smaller and the values of Cook's distance are inferior to 1 (see Fig. 18b). This validates the regression model described by Eq. (4) in OAGCMs and emphasizes its suitability at explaining the double ITCZ bias through both THR-MLT and CPCE indices.

[2] LOESS denotes a method that is also known as locally weighted polynomial regression. At each point in the data set a low-degree polynomial is fitted to a subset of the data, with explanatory variable values near the point whose response is being estimated. The polynomial is fitted using weighted least squares, giving more weight to points near the point whose response is being estimated and less weight to points further away.

References

Adler RF, Huffman GF, Chang A, Ferraro R, Xie P, Janowiak J, Rudolf B, Schneider U, Curtis S, Bolvin D, Gruber A, Susskind J, Arkin P, Nelkin E (2003) The version 2 global precipitation climatology project (GPCP) monthly precipitation analysis (1979-present). J Hydrometeorol 4:1147–1167

Arakawa A, Schubert WH (1974) Interaction of a cumulus cloud ensemble with the large-scale environment, part I. J Atmos Sci 31:674–701

Back L, Bretherthon C (2008) On the relationship between sst gradients, boundary layer winds and convergence over the tropical oceans. J Clim 22:4182–4196

Bacmeister JT, Suarez MJ, Robertson FR (2006) Rain reevaporation, boundary layerconvection interactions, and pacific rainfall patterns in an AGCM. J Atmos Sci 63:3383–3403

Bellon G, Gastineau G, Ribes A, Le Treut H (2010) Analysis of the tropical climate variability in a two-column framework. Clim Dyn 37:73–81

Bellucci A, Gualdi S, Navarra A (2010) The double-ITCZ syndrome in coupled general circulation models: the role of large-scale vertical circulation regimes. J Clim 5:1127–1145

Betts AK (1986) A new convective adjustment scheme. Part I: observational and theoretical basis. Quart J R Meteorol Soc 112:677–691

Bony S, Dufresne JL, Le Treut H, Morcrette JJ, Senior C (2004) On dynamic and thermodynamic components of cloud changes. Clim Dyn 22:71–86

Bougeault P (1985) A simple parametrisation of the large scale effects of cumulus convection. Mon Weather Rev 4:469–485

Charney JG (1971) Tropical cyclogenesis and the formation of the ITCZ. In: Reid WH (ed) Mathematical problems of geophysical fluid dynamics. American Mathematical Society, Providence, pp 355–368

Chikira M (2010) A cumulus parameterization with state-dependent entrainment rate. part II: impact on climatology in a general circulation model. J Atmos Sci 67:2194–2211

Chikira M, Sugiyama M (2010) A cumulus parameterization with state-dependent entrainment rate. Part I: description and sensitivity to temperature and humidity profiles. J Atmos Sci 67:2171–2193

Cook RD, Weisberg S (1982) Residuals and influence in regression. Chapman and Hall, New York

Dai AG (2006) Precipitation characteristics in eighteen coupled climate models. J Clim 9:4605–4630

De Szoeke SP, Xie SP (2008) The tropical eastern pacific seasonal cycle: assessment of errors and mechanisms in IPCC AR4

coupled ocean–atmosphere general circulation models. J Clim 21:2573–2590
Del Genio AD, Yao MS (1993) Efficient cumulus parameterization for long-term climate studies: the GISS scheme. American Meteorological Society, Providence, pp 181–184
Derbyshire SH, Maidens AV, Milton SF, Stratton RA, Willett MR (2011) Adaptive detrainment in a convective parametrization. Quart J R Meteorol Soc 137:1856–1871
Emanuel KA (1991) A scheme for representing cumulus convection in large-scale models. J Atmos Sci 48:2313–2329
Emanuel KA (1994) Atmospheric convection. Oxford University Press, Oxford
Fox J (2002) Nonparametric regression: appendix to an r and s-plus companion to applied regression. Sage Publications, Thousand Oaks, CA
Geoffroy O, Saint-Martin D, Olivié DJL, Voldoire A, Bellon G, Tytéca S (2012) Transient climate response in a two-box 1 energy-balance model. part I: analytical solution and parameter calibration using CMIP5 AOGCM experiments. J Clim 26:1841–1857
Gill AE (1980) Some simple solutions for heat-induced tropical circulation. Quart J R Meteorol Soc 106:447–462
Graham NE, Barnet TP (1987) Sea surface temperature, surface wind divergence, and convection over tropical ocean. Science 238:657–659
Grandpeix JY, Lafore JP (2010) A density current parameterization coupled with emanuel's convection scheme. Part I: the models. J Atmos Sci 67(4):881–897
Grandpeix JY, Lafore JP, Cheruy F (2010) A density current parameterization coupled with emanuel's convection scheme. Part II: 1d simulations. J Atmos Sci 67(4):898–922
Gregory D, Rowntree PR (1990) A mass flux convection scheme with representation of cloud ensemble characteristics and stability dependent closure. Mon Weather Rev 118:1483–1506
Gutzler DS, Wood TM (1990) Structure of large-scale convective anomalies over the tropical oceans. J Clim 3:483–496
Hess PG, Battisti DS, Rasch PJ (1993) Maintenance of the inter-tropical convergence zones and the tropical circulation on a water-covered earth. J Atmos Sci 50:691–713
Hirota N, Takayabu YN, Watanabe M, Kimoto M (2011) Preciptation reproducibility over tropical oceans and tis relationship to the double ITCZ problem in CMIP3 and MIROC5 climate models. J Clim 24:4859–4873
Holton JR, Wallace JM, Young JA (1971) On boundary layer dynamics and the ITCZ. J Atmos Sci 28:275–280
Hubert LF, Krueger AF, Winston JS (1969) The double intertropical convergence zone-fact or fiction? J Atmos Sci 26:771–773
Hwang YT, Frierson DMW (2013) Link between the double-intertropical convergence zone problem and cloud biases over the southern ocean. Proc Natl Acad Sci. doi:10.1073/pnas.1213302110
Lau KM, Wu HT, Bony S (1997) The role of large scale atmospheric circulation in the relationship between tropical convection and sea surface temperature. J Clim 10:381–392
Lin JL (2007) The double-ITCZ problem in IPCC AR4 coupled GCMs: ocean–atmosphere feedback analysis. J Clim 18:4497–4525
Lindzen RS (1974) Wave-CISK in the tropics. J Atmos Sci 31:156–179
Lindzen RS, Nigam S (1987) On the role of the sea surface temperature gradients in forcing the low-level winds and convergence in the tropics. J Atmos Sci 44:2418–2436
Liu H, Lin P, Yu Y, Zhang X (2012) The baseline evaluation of LASG/IAP climate system ocean model (LICOM) version 2. Acta Meteor Sinica 26:318–329
Liu Y, Guo L, Wu G, Wang Z (2010) Sensitivity of the ITCZ configuration to cumulus convective parametrizations on an aquaplanet. Clim Dyn 34:223–240
Mechoso CR, Robertson AW, Barth N, Davey MK, Delecluse P, Gent PR, Ineson S, Kirtman B, Latif M, Le Treut H, Nagai T, Neelin JD, Philander SGH, Polcher J, Schopf PS, Stockdale T, Suarez MJ, Terray L, Thual O, Tribbia JJ (1995) The seasonal cycle over the tropical pacific in coupled ocean–atmosphere general circulation models. Mon Weather Rev 123:2825–2838
Moorthi S, Suarez MJ (1992) The relaxed Arakawa-Schubert. A parametrization of moist convection for general circulation models. Mon Weather Rev 120:978–1002
Neale RB, Richter JH, Jochum M (2008) The impact of convection on ENSO: from a delayed oscillator to a series of events. J Clim 21:5904–5924
Nordeng TE (1994) Extended versions of the convection parametrization scheme at ECMWF and their impact upon the mean climate and transient activity of the model in the tropics. ECMWF Tech Memo No 206
Numaguti A (1993) Dynamics and energy balance of the Hadley circulation and the tropical precipitation zones: significance of the distribution of evaporation. J Atmos Sci 50:1874–1887
Oueslati B, Bellon G (2013a) Tropical precipitation regimes and mechanisms of regime transitions: contrasting two aquaplanet general circulation models. Clim Dyn 40:2345–2358
Oueslati B, Bellon G (2013b) Convective entrainment and large-scale organization of tropical precipitation: sensitivity of the CNRM-CM5 hierarchy of models. J Clim 26:2931–2946
Pan DM, Randall DA (1998) A cumulus parametrization with a prognostic closure. Quart J R Meteorol Soc 124:949–981
Rayner NA, Parker DE, Horton EB, Folland CK, Alexander LV, Rowell DP, Kent EC, Kaplan A (2003) Global analyses of sea surface temperature, sea ice, and night marine air temperature since the late nineteenth century. J Geophys Res Atmos 108:4407
Richter JH, Rasch PJ (2008) Effects of convective momentum transport on the atmospheric circulation in the community atmosphere model, version 3. J Clim 21:1487–1499
Song XL, Zhang GJ (2009) Convection parameterization, tropical pacific double ITCZ, and upper-ocean biases in the NCAR CCSM3. Part I: Climatology and atmospheric feedback. J Clim 22:4299–4315
Xie S, Hume T, Jakob C, Klein SA, MacCoy RB, Zhang M (2010) Observed large-scale structures and diabatic heating and drying profiles during TWP-ice. J Clim 23:57–79
Zhang C (2001) Double ITCZs. J Geophys Res Atmos 106(11):11,785–11,792
Zhang GJ, McFarlane NA (1995) Sensitivity of climate simulations to the parameterization of cumulus convection in the Canadian Climate Center general circulation model. Atmos Ocean 33:407–446
Zhang GJ, Mu M (2005) Effects of modifications to the zhang-mcfarlane convection parameterization on the simulation of thetropical precipitation in the national center for atmospheric research community climate model, version 3. J Geophys Res Atmos 110(D09):109